THE ASTROPHYSICAL JOURNAL, 273:105–127, 1983 October 1

SPECTRAL EVOLUTION OF GALAXIES. I. EARLY-TYPE SYSTEMS

GUSTAVO BRUZUAL A.
Centro de Investigaciones de Astronomía, Mérida, Venezuela
Received 1982 December 15; accepted 1983 March 21

ABSTRACT

This work develops models for the spectral evolution of early-type galaxies using population synthesis techniques. Different choices of the initial mass function and the star formation rate allow the construction of models which at the present epoch cover the range of observed galaxy spectra. Special emphasis is given to the ultraviolet region of the spectrum. Ultraviolet spectra of late-type stars and early-type galaxies obtained with the *International Ultraviolet Explorer* satellite are used in this work. The evolving spectral energy distributions are used to compute galaxy colors, magnitudes, *K*-corrections, and evolutionary corrections as functions of redshift for different photometric systems.

Subject headings: galaxies: evolution — galaxies: photometry — galaxies: stellar content — ultraviolet: spectra — stars: formation

I. INTRODUCTION

Galaxy evolution is a complicated subject which is usually approached from two different points of view. (1) Dynamical evolution involves the formation, collapse, and light and mass distribution of the resulting galaxy. These processes are only partially understood. In particular, it is not known at which stage in this evolution the morphological type of the resulting galaxy is determined. (2) Spectral evolution deals with the study of the stellar populations present in a galaxy as a function of time, and, hence, of its combined spectrum, luminosity, colors, and other observable features.

It is usually assumed that these two evolutionary processes occur independently. This is an artificial first-order approximation, since it is very likely that the dynamical evolution determines to a large extent the initial stages of star formation. Also, the fraction of a galactic mass that is transformed into stars at the very early phases of galaxy formation has important consequences for the subsequent dynamical evolution (stellar versus dissipative). Thus, both processes are interconnected, and they are separated just for convenience and owing to our lack of knowledge.

In this work I will study the spectral evolution of galaxies without reference to their dynamics, nor to their interactions with other galaxies or with the intergalactic medium; i.e., a galaxy will be considered a closed system.

Is there any evidence of spectral evolution in galaxies? There are two lines of thinking in looking for this evidence. (1) Theoretically: from studies of stellar structure and evolution we know that stars of mass greater than about 1 $m_\odot$ evolve during lifetimes shorter than the estimated age of galaxies. This produces a continuous change in the relative numbers of stars at different evolutionary stages, which translates into differences in the galaxy spectrum at different epochs. For instance, if we accept the idea that the heavy elements are produced locally in galaxies and do not come from the primeval gas, we expect elliptical galaxies to have had large numbers of massive stars at their early epochs (the ones that are responsible for producing these elements). These stars are expected to contribute mostly in the ultraviolet region of distant elliptical galaxies. (2) Empirically: observed differences between the spectral energy distributions (s.e.d.'s) of galaxies that are supposedly identical but seen at different ages, i.e., different redshifts, can be interpreted as evidence for spectral evolution (Spinrad 1977, 1980; Wilkinson and Oke 1978; Bruzual 1981*a*; Bruzual and Spinrad 1981). However, it is difficult to distinguish these differences from the ones produced by random star formation events (as may happen in interacting elliptical galaxies in clusters of galaxies) or by slightly different populations present in the galaxies (e.g., differences in the horizontal-branch population). Additionally, known color and metallicity gradients present in galaxies can conspire in such a way as to mimic an evolving population: through a given aperture only the nuclear regions of nearby galaxies are observed, whereas the same angular aperture covers the entire galaxy for more distant systems. This effect alone is sufficient to make the distant galaxy look bluer than the nearby one, independently of any degree of evolution.

The most common tool used to study the stellar content of galaxies is spectral synthesis. Two independent synthesis techniques have been developed. (1) Population synthesis: This technique was introduced by Faber (1972) to improve the trial and error method used up till then (Spinrad and Taylor 1971). In this method the s.e.d. of a galaxy is represented as a linear combination of the s.e.d.'s of as many stellar types as desired. The best model is chosen objectively by minimizing a function, typically the sum of the residuals squared. This method has been employed successfully by several authors (Faber 1972;

O'Connell 1976, 1980; Pritchet 1977; Turnrose 1976). To produce astrophysically sound models, constraints referring to various stellar groups must be introduced (e.g., the number of stars must be positive, the number of stars in the main sequence must increase with decreasing stellar mass, the number of giant stars must be consistent with the number of their progenitors, etc.). The quality of the observational data being used (star and galaxy s.e.d.'s) must be comparable in order to get meaningful models and must be free from systematic errors introduced by poor data in some wavelength range. (2) Evolutionary synthesis: In this approach, started by Tinsley (1967, 1972*a*), analytical expressions are assumed for both the star formation rate and the initial mass function. These two functions give the number of stars of a given mass born during a given time interval. Evolutionary tracks indicate the amount of time spent by stars of different masses at different positions on the H-R diagram. Models for a single generation of star formation or a continuous star formation rate can be built. Once the stellar population content of a model is calculated, the predicted spectrum is easily found. Comparison of the observed galaxy spectrum with these model spectra provides estimates of the galaxy age. Since the evolutionary history of the stellar population up to that age is known, it is possible to make predictions about how the galaxy spectrum looked at a previous epoch.

Clearly, the evolutionary synthesis approach proves itself more convenient for the study of spectral evolution, and it is the one used in this investigation. Population synthesis does not provide us with any information about how the stellar content of a galaxy came to be what the model predicts, and there is no unique way to derive its past evolution. In this particular case, the ultraviolet data for galaxies are of much lower quality than those for stars, making population synthesis less reliable in this range.

Several attempts have been made in the past (Tinsley 1972*b*, 1977, 1980*a*, *b*) to apply the evolutionary synthesis approach to the understanding of the spectral evolution of galaxies. These early studies have provided theoretical predictions that are in close enough agreement with observational data to justify further work along the same lines.

Previous efforts have been limited to the prediction of the time dependence of broad-band fluxes and colors in the optical region of the spectrum. These models, together with some choice of the cosmology and the observed galaxy luminosity function, allowed the construction of theoretical Hubble diagrams and galaxy count versus magnitude diagrams in the appropriate bandpasses up to moderate redshifts. The lack of observational data on galaxies outside the traditional *B*, *V*, *R* photoelectric system discouraged workers from exploring the full spectral range. However, new developments have occurred recently that make it possible and desirable to extend the previous scheme to cover the whole spectrum. These developments are (1) Ultraviolet s.e.d.'s for nearby galaxies (especially elliptical galaxies) and for stars of most spectral types have become available, as ultraviolet detectors have been launched on board various satellites (*ANS*, *OAO 2*, *IUE*). (2) Ground-based observations of the brightest galaxy in distant clusters (Spinrad 1977; Gunn and Oke 1975) have provided reasonably good s.e.d.'s up to $z > 0.6$ (look-back time of 7 or 3.5 Gyr for $q_0 = 0$, $H_0 = 50$ or 100, respectively). (3) High-quality photographic surface photometry of complete samples of faint galaxies in several bandpasses have become available (Kron 1980, and references therein; Koo 1981*a*; van der Laan and Windhorst 1982*a*, *b*). Interpretation of these counts and their color distribution (Bruzual and Kron 1980, hereafter BK; Koo 1981*a*, *b*) suggests that a large fraction of these galaxies is situated at $z > 0.5$, involving, again, fairly large look-back times. (4) Finally, at the other end of the spectrum, infrared magnitudes and colors of galaxies are now being measured (Persson, Frogel, and Aaronson 1979; Lebofsky 1980; 1981; Grasdalen 1980). Comparing evolution at both ends of the spectrum, it is possible to perform a consistency check in the evolutionary models, especially because at infrared wavelengths evolution is much slower than in the ultraviolet.

These observational data provide enough constraints to test models for spectral evolution of galaxies. Comparison of the observed spectra and colors with the model predictions at different epochs allows us to derive conclusions about functions like the star formation rate, or the initial mass function, or parameters like the galaxy age (once a value of H_0 is chosen).

This paper is the first of a series in which I present results obtained as part of an ambitious project that involves the study of the spectral evolution of galaxies of all morphological types in the wavelength range from the ultraviolet to the infrared. The elaboration of these spectral evolutionary models has been a long-term project. The current generation of models supersedes three of four previous generations. Since the first generation of models was finished (late 1978), I have had the opportunity to compare the predictions of the models with observations obtained by different groups. Detailed comparisons of faint-galaxy number counts and color and redshift distributions have appeared in Kron (1978), BK, Bruzual (1981*a*), Gunn (1982), and, especially, Koo (1981*a*, *b*).

The latest generation of these models (Bruzual 1981*a*) was made available to several groups actively working in the fields of faint-galaxy photometry and spectrophotometry. Some of these groups have performed their own comparisons of their data with the model predictions. Thus, the colors of faint radio galaxies have been investigated by van der Laan and Windhorst (1982*a*, *b*; 1983*a*, *b*), by Lilly and Longair (1982), and by Lilly, Longair, and McLean (1983). Comparisons of model spectral energy distributions and *IUE* spectra of nearby spheroidal galaxies (including both elliptical galaxies and central bulges of spiral galaxies) have been presented by Bruzual (1981*a*), Bruzual and Spinrad (1981), and Bruzual, Peimbert, and Torres-Peimbert (1982). The implications of this galaxy evolutionary

scheme for the predicted spectrum of the extragalactic background light have been considered by Bruzual (1981*b*) and Code and Welch (1982).

Needless to say, these comparisons have increased considerably our knowledge about the models, their limitations, and range of applicability. From the work of Koo (1981*a*, *b*) it has become apparent that the models intended to represent present-day blue galaxies, i.e., systems in which star formation is currently taking place in appreciable amounts, are not as successful as redder models. Specifically, the agreement between the predicted and observed ultraviolet s.e.d.'s of nearby spiral galaxies of a given optical color is not well established. The scarcity of observations of this kind, as well as the large differences observed from galaxy to galaxy, makes it difficult to choose the region of parameter space in which the models best representing spiral galaxies lie. This situation should improve in the near future as more ultraviolet spectra of spiral galaxies are obtained, both by *IUE* and, especially, by the Space Telescope. The models appropriate for late-type systems will be the subject of a separate investigation.

Section II describes the approach used and the auxiliary data needed to construct the models. In §§ III and IV, model results are compared with data available for nearby elliptical galaxies and first-ranked distant cluster galaxies. Predictions are presented for quantities of interest up to $z \sim 1$. The conclusions are presented in § V.

II. MODELS

The purpose of this investigation is to construct models for the spectral evolution of galaxies that are detailed enough to provide (1) galaxy spectra with sufficient resolution to allow the computation of arbitrary broad-band magnitudes and colors, and (2) evolution in time of these spectra, with small enough time steps to allow accurate interpolation at any redshift.

The discussion below follows the one in BK. Part of it is repeated here for reasons of completeness and in order to establish a uniform notation to be used in this series of papers.

a) Analytical Scheme

In the evolutionary synthesis approach, analytical expressions are assumed for the initial mass function (IMF) and the star formation rate (SFR). A model is then specified by the values assigned to the parameters appearing in these functions. Usually the IMF is assumed to be a function of the stellar mass only (and some parameter x), whereas the SFR is taken as a function of time (and a time scale τ). This is an approximation, since in reality both dependences may be interrelated.

The number of stars formed per unit mass and per unit time is represented as

$$S(m, x)R(t, \tau) . \quad (1)$$

The following parametric representations have been considered in this study.

i) *Initial Mass Function*

It is assumed that at all times stars form in the mass range $m_s < m < m_u$ with a Salpeter-like mass spectrum,

$$S(m, x) = S_0(x)m^{-(1+x)} , \quad (2)$$

where $S(m, x)$ is the fraction of stars of mass m formed per unit mass range, and $S_0(x)$ is a normalization factor, given by

$$S_0(x)^{-1} = \int_{m_l}^{m_u} m^{-(1+x)}dm .$$

Objects in the range $m_l < m < m_s$ do not become luminous stars but are included to guarantee an appropriate mass-to-light ratio. The present models were computed with $(m_l, m_s, m_u) = (0.05, 0.08, 75)m_\odot$. For the solar neighborhood Salpeter (1955) found $x = 1.35$. Discussions with Dr. R. Green have suggested that the population of white dwarfs in the solar neighborhood may indicate a value as high as $x = 1.70$. A range of x has been considered in the models, but it should be pointed out that a single value of x may be unrealistic in its representation of the true stellar mass distribution (Tinsley 1980*a*; Serrano 1978).

ii) *Star Formation Rate*

A galaxy is considered to be a closed system of mass M_0. A characteristic time scale for galaxy evolution is introduced through the SFR. Two different expressions for the SFR have been used in this study.

$$\text{Constant: } R(t, \tau) = \frac{M_0}{\tau} , \quad 0 \le t \le \tau . \quad (3)$$

No star formation takes place for $t > \tau$.

$$\text{Exponential: } R(t, \tau) = \frac{M_0}{\tau} \exp\left(\frac{-t}{\tau}\right) . \quad (4)$$

In both cases $R(t, \tau)$ represents the mass of gas transformed into stars per unit time. The normalization in equation (3) is such that the whole system becomes stars after a time τ. In equation (4) an infinite time is required, i.e.,

$$\int_0^\infty R(t, \tau)dt = M_0 .$$

Note that according to equation (4), $R(t, \tau)$ is maximum at $t = 0$. For both SFRs it is assumed that the gas returned by dying stars is transformed again into stars. Thus, the total mass of material processed in stars is larger than M_0. For convenience, the parameter

$$\mu = 1 - \exp(-1 \text{ Gyr}/\tau) \quad (5)$$

is used in the exponential SFR. The quantity μ represents the fraction of M_0 that would be in stars after $t = 1$ Gyr, if dying stars did not return gas. Values of μ in the range 0.01–0.95, corresponding to 99.5–0.33 Gyr in τ, have been considered. The results will be labeled with the appropriate value of μ, and equation (5) should allow a comparison of the present models with those of other

authors who use τ as a parameter, e.g., Searle, Sargent, and Bagnuolo (1973), Huchra (1977), and Tinsley (1980*b*). Models with SFRs given by equations (3) and (4) will be denoted as c- and μ-models, respectively.

iii) *Procedure*

The procedure used to construct the models is as follows. The mass that is transformed into stars during the time interval $\Delta t = t_2 - t_1$ is

$$\Delta M(t_1, t_2) = \int_{t_1}^{t_2} R(t, \tau) dt \, . \quad (6)$$

The number of main sequence stars of mass m_j formed out of ΔM is given, according to equations (1) and (2), by

$$N(m_j, t_1, t_2) = S_0(x) \Delta M(t_1, t_2) \int_{m_1}^{m_2} m^{-(1+x)} dm \, , \quad (7)$$

where $m_j, j = 1, 2, \ldots, n$, is one of the masses for which an evolutionary track starting in the main sequence is available ($m_j > m_{j+1}$), and

$$m_1 = (m_j m_{j-1})^{1/2} \, , \quad m_2 = (m_{j+1} m_j)^{1/2} \, ,$$

as in Tinsley (1972*a*). To distribute the stars of mass m_j along the different stages in their evolutionary track the following scheme was used. Let us assume that the stars of mass m_j live in their kth evolutionary stage from time T_i to time T_f. When the N stars given by equations (6) and (7) are observed at time T, they will have ages ranging from $T - t_2$ to $T - t_1$. The number of these stars that have reached, or are still in, the kth stage by time T is proportional to the number of them born during a time period equal to the intersection of the time intervals (T_i, T_f) and $(T - t_2, T - t_1)$. Analytically, the fraction of stars in the kth stage at time T is given by

$$f_j^k(T) = \frac{\Delta M(T_1, T_2)}{\Delta M(t_1, t_2)} \, , \quad (8)$$

where $T_1 = \max(T_i, T - t_2)$, and $T_2 = \min(T - t_1, T_f)$. When $T_i \geq T - t_1$, or $T_f \leq T - t_2$, $f_j^k(T)$ is equal to zero. After a star lives through the last stage in the track, it becomes one of three possible remnants (see below). At a given time, the total number of stars in a given evolutionary stage is obtained by adding the corresponding numbers of stars, given by equations (7) and (8), formed up to that time in successive time steps. At every time step the galaxy spectrum is computed by adding the stellar spectra corresponding to the different positions in the H-R diagram, weighted according to the number of stars in each position.

b) Evolutionary Tracks

Table 1 lists the stellar masses and the references from which the respective evolutionary tracks have been obtained. For stellar masses larger than 2 $m_\odot$ the tracks were interpolated in the log L–log $T_{\rm eff}$ plane to the solar composition, assumed to be $(X, Y, Z) = (0.71, 0.27, 0.02)$. For the Ciardullo and Demarque (1977) CD-tracks, a different interpolation scheme was used. Their compilation contains tracks for $Y = 0.20, 0.30$; $Z = 0.01, 0.04$. Plots of log $M_T(t)$ versus log Z were constructed from their tables for $Y = 0.20$ and 0.30. The quantity $M_T(t)$ represents the mass of the stars approaching the tip of the red-giant branch at age t. From these plots, the values of log Z corresponding to a given set of masses at different ages were read. A fourth-degree polynomial in log Z and $M_T(t)$ was fitted to the Z, $M_T(t)$, and t data table for both values of Y. Then, fixing the value of Z to 0.02, the polynomial allowed the computation of the masses approaching the tip of the red-giant branch at any age for this value of Z. The tracks for these masses were then interpolated quadratically from the tracks in the CD-tables to the desired chemical composition. This interpolation scheme was checked by comparing the derived track for a 1 $m_\odot$ star with that of Iben (1967). The agreement was considered satisfactory.

TABLE 1

SOURCE OF EVOLUTIONARY TRACKS FOR DIFFERENT MASSES

Mass ($m_\odot$)	Reference
60, 40, 30, 20	Chiosi *et al.* 1978
10, 7, 5, 2	Alcock and Paczyński 1978
3, 2.25	Iben 1967
34 masses in the range 1.9–0.8	Ciardullo and Demarque 1977
0.69–0.08 (unevolving)	Tinsley and Gunn 1976

No chemical evolution has been considered. This is a good approximation since the mean metallicity of the stars quite rapidly approaches the yield (see, e.g., Searle 1972). From the observational point of view, the spectrum of distant elliptical galaxies ($z \sim 0.5$) shows the characteristic spectral features of an old metal-rich stellar population. These stars were formed with this metallicity at the time the galaxies were formed. Thus, the approximation of constant metallicity seems justified.

None of these evolutionary tracks extend beyond helium ignition. Stars more massive than 1.9 $m_\odot$ have been assumed to become (*a*) black holes of mass 8 $m_\odot$ if $m \geq 8$ $m_\odot$; (*b*) neutron stars of mass 2 $m_\odot$ if 2.5 $m_\odot \leq m < 8$ $m_\odot$; and (*c*) white dwarfs of mass min $(1.4, m - 0.2)$ if $m < 2.5$ $m_\odot$, as soon as the last evolutionary stage in the track is finished. The gas returned by dying stars of all masses is added to the remaining gas.

For stars of $m < 1.7$ $m_\odot$ the empirical giant luminosity function of Tinsley and Gunn (1976) with the short clump lifetime and the two last time steps revised to 0.032×10^7 yr (case R2 in Tinsley 1978) has been used. All these stars are assumed to evolve into the same giant branch, with equal times spent at identical positions (irrespective of mass). This lack of a mass-luminosity relationship for giants (as observed) has the effect that models in which star formation takes place at early times will have similar spectra and colors at the present time for any slope of the IMF. In addition, the time evolution of the spectra will be insignificant. The rate at which the giant branch is populated does depend on x, and thus so does the luminosity evolution

of the galaxy. For c-models with $\tau = 1$ Gyr, we have $dM_V/d \log t_9 = 1.30 - 0.30x$, for $t_9 = t(\text{in Gyr})/10^9 > 2$, which agrees with Tinsley (1978).

The resulting evolutionary tracks are listed in Table 2 of Bruzual (1981*a*). The spectral type at each stage is also given. The theoretical H-R diagram was transformed to observational quantities as in Flower (1977). Table 3 of Bruzual (1981*a*) contains the look-up tables used for this purpose. These tables will not be repeated here for reasons of space, but they will be supplied to the reader upon request.

c) *Stellar Spectra*

The stellar s.e.d.'s were taken from the references given in Table 2, which also gives the spectral resolution. All these data are already published, except for the *International Ultraviolet Explorer* (*IUE*) data acquired or compiled by the author. Table 3 lists the stars, spectral types, and long wavelength redundant (LWR) image number for which *IUE* data was obtained. For spectral types or stars with more than one entry in this table an average spectrum was used after normalization at $\lambda = 2940$ Å. These *IUE* spectra in the range 2000–3240 Å are presented in Figure 1 of Bruzual (1981*a*) as plots of F_λ versus λ, and in his Table 6 the spectra are listed in numerical form. These data are repeated in Bruzual (1983*a*, hereafter Paper II). For the stellar types for which a spectrum was not available, a linear interpolation was performed between the two (if in the same luminosity class) or four (if for an intermediate luminosity class) bracketing spectra.

d) *Additional Data*

Throughout this work, observational data in several broad-band color systems (photoelectric and photographic) will be compared with model predictions. This requires knowledge of the filter response functions and the zero points for the given color. The magnitude of a source with s.e.d. $F_\lambda(\lambda)$ at zero redshift observed through a filter of response function $R(\lambda)$ is given by

$$C - 2.5 \log \int_{-\infty}^{\infty} F_\lambda(\lambda) R(\lambda) d\lambda \,, \qquad (9)$$

where C is a constant that defines the magnitude system.

TABLE 2

STELLAR SPECTROPHOTOMETRY

Wavelength (Å)	Resolution (Å)	Reference
240–1200	20	Kurucz 1979[a]
1200–3600	20	Code and Meade 1979[b]
2000–3300	5	*IUE* data from author[c]
3300–10000.....	50	Straižys and Sviderskiene 1972
>10000	[d]	Johnson 1966

[a] Model atmospheres.
[b] For stars earlier than G2.
[c] For stars later than G2.
[d] Broad-band fluxes.

TABLE 3

STARS OBSERVED WITH *IUE*

Sp. Type	Star	LWR Image No.
F0 III	γ Tuc	4688
G2 V	Sun	[a]
	16 Cyg A	1888, 1889
G5 III	ι Tuc	4689
G7 III	λ^2 Tuc	4690
G8 III	ϵ And	4670
	η And	4671
	λ And	4666
K0 III	α Cas	4646
	3 And	4667, 4668
K1 III	β Cet	4672, 4687
K3 III	δ And	4669
K4 III	ϕ^3 Cet	4686
K5 III	δ Psc	4684, 4685
M0 III.....	β And	4683

[a] The data for the Sun were taken from Broadfoot 1972 and Arvesen, Griffin, and Pearson 1969.

Table 4 lists the color systems, filter characteristics, and the references from which the functions $R(\lambda)$ were obtained. The photographic U and J bands are denoted U^+ and J^+ to differentiate them from the U band of the *UBV* system and the J band of the *RIJHKL* system, respectively. The filter response functions are listed in Table 8 of Bruzual (1981*a*). See Koo (1981*a*) for a revised version of the U^+ response function.

For all the synthetic colors computed in this work, the zero points were established from the spectrum of an A0 V star; i.e., this star was required to have all colors = 0, taken from Straižys and Sviderskiene (1972). In the ultraviolet the *OAO 2* spectrum of α Lyrae was used.

Similarly, frequent use will be made of cosmological expressions. Friedmann cosmological models with zero cosmological constant have been used. In the remainder of this work, time will be measured in Gyr, and H_0 in km s^{-1} Mpc^{-1}. In both cases the units will not be indicated. For time, the following notation will be used. The age of the universe will be denoted by t_0, the age of the galaxies by t_g, and the current value of time by t. As before, τ will always refer to the time scale appearing in the SFR.

III. GENERAL RESULTS

A galaxy spectral evolutionary model consists of a series of from 28 to 32 s.e.d.'s going from $t = 0.001$ to $t = 20$. This section contains some examples of general properties of the models. Some of these results have been presented already in BK and will be mentioned here only briefly.

Figure 2 of BK shows the position in the UBV-plane of several models at $t = 16$. The observational envelope is taken from Huchra (1977). The μ-models shown in this figure were constructed with $x = 1.35$ in the SFR. The c-model ($\tau = 1$) is not shown because it coincides with the reddest point for the μ-models. The μ-models

TABLE 4

PHOTOMETRIC SYSTEMS

System	Colors	Filters	λ_{eff} (Å)	$\Delta\lambda$ (Å)
UBV[a]	$U-B=U_3-B_2$	U_3	3652	201
	$B-V=B_3-V$	B_2	4448	363
		B_3	4417	362
		V	5505	367
U^+J^+FN[b]	U^+-J^+	U^+ = IIIa-J+UG5	3606	223
	J^+-F	J^+ = IIIa-J+GG385	4627	487
	$F-N$	F = 127-02+GG495	6167	599
		N = IV-N+RG695	7941	562
$RIJHKL$[c]	$V-R$	R	6940	754
	$V-K$	I	8781	869
	$J-K$	J	12488	1198
	$H-K$	H	16500	879
		K	21951	1772
		L	34371	2354
ST[d]	14−17	B 140	1405	120
	17−22	B 175	1751	166
	22−27	B 220	2200	210
	27−B, 27−V	B 275	2750	252

NOTE: $\lambda_{eff}=\frac{\int_{-\infty}^{\infty}\lambda R(\lambda)d\lambda}{\int_{-\infty}^{\infty}R(\lambda)d\lambda}$, $(\Delta\lambda)^2=\frac{\int_{-\infty}^{\infty}(\lambda-\lambda_{eff})^2R(\lambda)d\lambda}{\int_{-\infty}^{\infty}R(\lambda)d\lambda}$.

[a] Ažusienis and Straižys 1969; Buser 1978.
[b] Kron 1978; D. C. Koo and R. G. Kron 1980, private communication.
[c] Johnson 1965; Lebofsky 1980, private communication.
[d] Macchetto *et al.* 1980; G. Djorgovski 1980, private communication.

with $\mu > 0.6$ are by the present epoch ($t > 10$) very similar to the c-models with $\tau = 1$ (since the residual star formation is very low). On the other hand, μ-models with $\mu \ll 1$ have a practically constant SFR and a very low rate of gas consumption. For example, at $t = 16$ for a $\mu = 0.01$ model with $x = 1.35$, we have $M_{gas} = 0.90\ M_0$ and SFR of 0.86 $m_\odot$ yr^{-1}. The exponential SFR (eq. [4]) is highest at $t = 0$. This has the effect of producing a relatively large number of low-mass stars ($m < 1\ m_\odot$) at early epochs in the life of the galaxy. The evolution of these stars into red giants by the present time tends to make these models not as blue as the bluest normal galaxies observed. Assuming lower values of μ does not change the situation as long as $x > 1$.

The d-models (see BK and Bruzual 1981*a*) have the advantage of starting with a low SFR, which reduces the number of low-mass stars formed at early epochs. This allows large values of the SFR (at all later times) and, hence, blue systems with a more realistic gas mass to total mass ratio at the present time (Roberts 1975). For example, a d-model with $\tau = 10$ will have at $t = 16$, $M_{gas} = 0.52\ M_0$ and SFR = 3.2 $m_\odot$ yr^{-1}. Given the belief that star formation occurs more efficiently in regions of high gas density, these models should be appropriate for galaxies that start as very low density systems, for which there is no reason to expect that the SFR was maximum at $t = 0$.

To cover the range of observed colors shown in Figure 2 of BK, values of μ from 0.01 to 0.9 were used. With $x = 1.35$ it is not possible to produce models that at $t = 16$ are bluer than $B-V = 0.5$, $U-B = -0.1$ for either μ- or d-models. The evolution in time of a given model is such that in this plane the colors describe a line parallel to the set of points shown in the figure. Thus one possible choice for the bluer galaxies is to choose the same model as for redder systems but assume a younger age for the former. The choice of models presented allows the range of observed colors to be covered with models of the same age and metallicity.

We remark that these results still hold for a younger present age, e.g., $t_g = 10$–12, even though the particular choice of parameters may change. It should also be noted that we are assuming that star formation occurs continuously. If stochastic bursts of star formation occur in galaxies of any type, these galaxies will look much bluer just after the episode than their average past history of star formation would imply.

Other results of interest for the present investigation are shown in Figures 3 and 4 of BK. Figure 3 shows the bolometric luminosity as a function of time for several representative models. In Figure 4 the predicted $B-V$ and $V-R$ colors as a function of redshift (z) for several models are compared with the Kristian, Sandage, and Westphal (1978) BVR photometry of first-ranked cluster galaxies. See BK and the following sections for more details on this comparison.

Since in this paper I will consider models appropriate for early-type systems, no more reference will be made to d-models.

IV. MODELS FOR EARLY-TYPE SYSTEMS

The visual spectrum of elliptical galaxies and of central bulges of early-type spiral galaxies is dominated by late-type giant stars (from about G8 III to K2 III). The semiempirical giant luminosity function of Tinsley and Gunn (1976) was constructed to reproduce the spectrum of this type of population. Thus we expect our evolutionary models to reproduce this early-type galaxy spectrum only when the dominating population is the giant group. This occurs at $t \sim 10$ for the c-model ($\tau = 1$) and at $t \sim 10$–11 for μ-models with μ in the range 0.6–0.9, corresponding to τ in the range 0.4–1.1 in equation (4). The residual star formation in the latter models is small enough that the spectrum is not different from that of an old population. This result should not be taken to imply that elliptical galaxies are undergoing star formation, but rather it is an artifact of the modeling technique. As expected, the differences increase at ultraviolet (UV) wavelengths, and the μ-models agree better with the observed spectra than the c-model. This is because the main-sequence stars in the μ-models are producing the blue light that is known to be missing in the c-models with only the lower main-sequence and the red giant–branch stars (Wu *et al.* 1980; Bruzual and Spinrad 1981). These main-sequence stars mimic the horizontal-branch (HB) stars that are present in the galaxies but are lacking in the models.

a) *Spectral Evolution*

The evolving s.e.d.'s for a c-model ($\tau = 1$) and a $\mu = 0.7$ model are shown in Figure 1 for different ages in the rest frame of the galaxy (for both models $x = 1.35$). Of interest is the very dark UV for the c-model and the relatively large flux in the same spectral region for the μ-model. In Figure 1*a* the fluxes below 2.5 log $F_\lambda = 8$ are artificial, being extrapolated smoothly to zero at short wavelengths (essentially due to the lack of data for late-type stars shortward of 2000 Å). The increase with time of the amplitude of the spectral discontinuity at 4000 Å is also clearly seen in Figure 1 (see § IV*b*).

The line marked "Obs." in Figure 1 shows the observed spectrum of a typical nearby elliptical galaxy. This has been constructed from Pence's (1976) mean elliptical galaxy s.e.d. (corrected for extinction in the Galaxy) for $\lambda > 3300$ Å and UV data obtained with *IUE* (also corrected for interstellar reddening in the Galaxy). A spectrum of M32 extending down to 3150 Å, kindly provided by T. Boroson, was used as a guide to join both s.e.d.'s. The reddening law (analytical approximation) from Seaton (1979) was used to correct the observed UV spectra. As in the optical, the degree of similarity among the UV spectra of different elliptical galaxies in the 2000–3200 Å region is very high, and it is possible to define a mean elliptical galaxy UV spectrum. The UV part of the observed spectrum shown in Figure 1 is the average of individual *IUE* spectra of M31 (bulge), M32, and NGC 4472. Different spectra were assigned weights in proportion to the observing time and in accord with spectral quality. None of these galaxies show the rapid increase shortward of 2000 Å that has been observed in NGC 4486 (Bertola *et al.* 1980; Perola and Tarenghi 1980) and NGC 4649 (Bertola, Capaccioli, and Oke 1982). The *IUE* data presented here are an improved version of the data presented in Bruzual and Spinrad (1981). The s.e.d. has been extended down to 1200 Å using observations of M31 and M32, and the number of independent exposures has been enlarged. The final reduction of the *IUE* spectra was performed by the author, based on the data provided by the *IUE* data reduction facilities. The final averages are shown in greater detail in Figure 7 of Bruzual (1981*a*) and Figures 1 and 2 of Bruzual, Peimbert, and Torres-Peimbert (1982). The first of these two references lists the spectrum in numerical form. These data are repeated in Paper II, as well as the details of the author's *IUE* reduction program. In these spectra the high-frequency noise should not be taken as spectral features. Most often these apparent emission peaks represent particles hitting the detector at any time during the exposure.

Comparison of the models shown in Figure 1 with the observed spectrum allowed the determination of the following results.

1. In the region from 2000 to 4000 Å the observed spectrum is well reproduced by models at $t = 5$, which still have F stars on the main sequence. However, at this age this model has $B-V = 0.82$, which is about 0.15 mag bluer than a typical giant elliptical. In addition the corresponding short look-back time would imply formation redshifts for $q_0 = 0$ of 0.34 ($H_0 = 50$) or 1.04 ($H_0 = 100$), which seem much too low for current views of massive galaxy formation. The predicted $B-V$ at $z = 0.46$ is 1.26 ($H_0 = 100$), which is too blue for the observed color of 1.4 (Kristian, Sandage, and Westphal 1978). For a different interpretation, see O'Connell (1980).

2. In the region from 5000 to 8000 Å, the observed spectrum is not reproduced until an age of about 10. However, by this time the models are very deficient in UV light. This deficiency can be traced back to the fact that some stellar group is missing in the stellar population used in the models. This is not surprising since the red-giant luminosity function of Tinsley and Gunn (1976) is based on optical and infrared data from nearby giant elliptical galaxies, and elliptical galaxies with almost identical optical and infrared spectra show large variations in the UV, shortward of 2000 Å (see, e.g., Bertola *et al.* 1980; Nørgaard-Nielsen and Kjaergaard 1981; Perola and Tarenghi 1980; Oke, Bertola, and Capaccioli 1981; Bertola, Capaccioli, and Oke 1982). This fact seems to indicate a bimodality in the stellar content distribution of these systems. Note that in Figure 1 the agreement with the observed spectrum is better for the μ-model, in which a slight amount of star formation is still going on, and some upper main-sequence stars are present.

Wu *et al.* (1980) have reviewed the possible sources of this UV light. They include (*a*) hot HB stars and blue stragglers in a metal-rich population, (*b*) HB stars

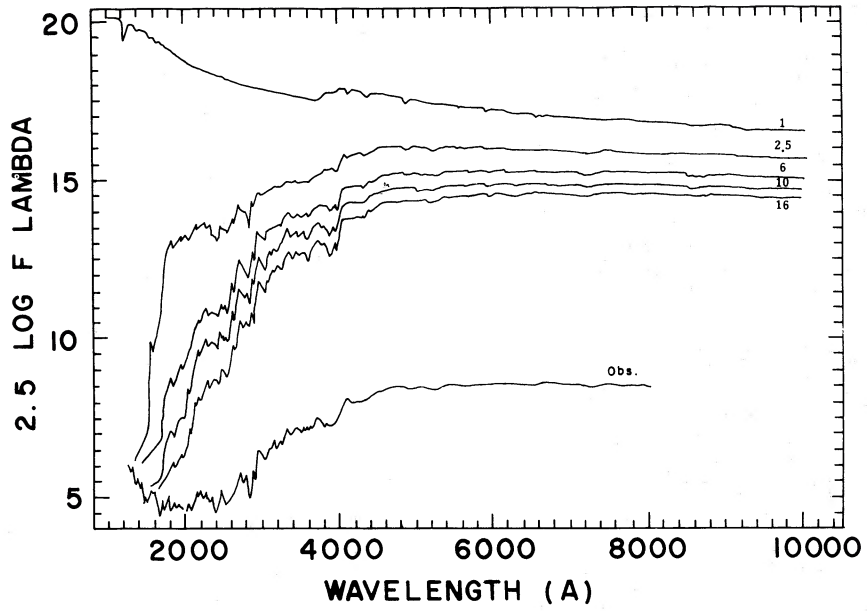

FIG. 1*a*

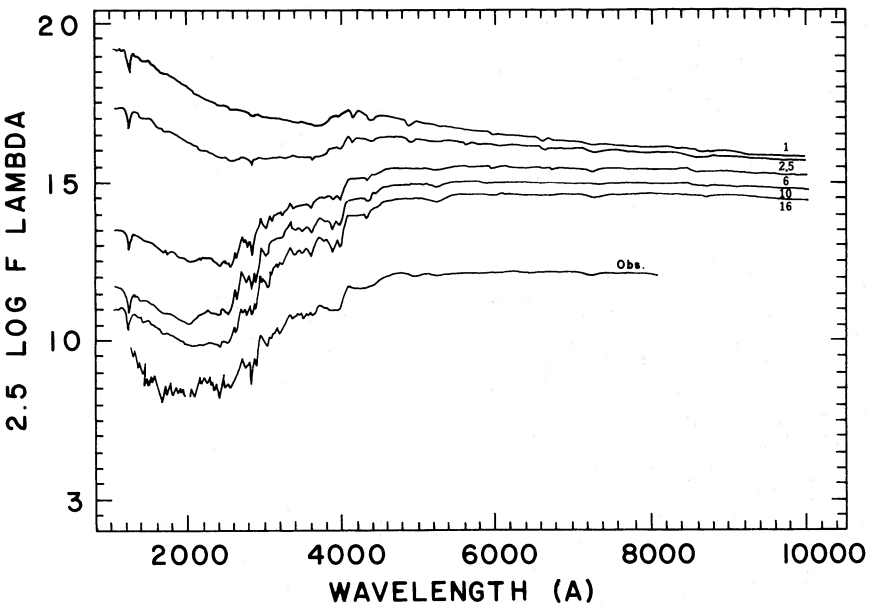

FIG. 1*b*

FIG. 1.—(*a*, *b*) Examples of evolving energy distributions; ages, in Gyr, are as indicated. Fig. 1*a* is the *c*-model ($\tau = 1$); Fig. 1*b* is a $\mu = 0.7$ model. Both models have $x = 1.35$. In Fig. 1*a* the fluxes below 2.5 log $F_\lambda = 8$ are artificial, being extrapolated smoothly to zero at short wavelengths. The line marked "Obs." represents the observed s.e.d., shifted arbitrarily in the vertical direction.

in a minority metal-poor component, (*c*) nuclei of planetary nebulae, (*d*) subdwarf O and B stars, (*e*) white dwarf stars. Even though all of these stars have the right temperature to emit appreciable amounts of light in the UV, the first two groups are the most plausible sources of the UV in elliptical galaxies. The number of planetary nebula nuclei required to reproduce the spectrum of M31 is larger than the number of these nebulae that can be counted in photographic surveys of this galaxy, according to Wu *et al.* This bright phase of the central stars of planetary nebulae is usually very short lived, which contributes to their apparent scarcity. The O and B subdwarfs are ruled out because of their unknown origin and the difficulty of justifying large numbers of them. White dwarfs cool too fast to be the major contributors of UV light (at most only 10% at 2500 Å, according to Wu *et al.*).

It seems then that HB stars, either metal-poor or

metal-rich ones, are the most likely candidates for the source of the UV light in an old stellar population. These stars are present in globular clusters in our Galaxy, as well as in the galactic halo (even though their identification as such is not an easy problem). The source of the UV light in elliptical galaxies seems to be a well-mixed population, with the same spatial distribution as the stars that are producing the optical and infrared emission (Bertola *et al.* 1980; Oke, Bertola, and Capaccioli 1981). This is expected from an HB population, as opposed to small-scale regions where star formation may be going on.

Alternatively, one may also assume that star formation is still going on in elliptical galaxies, and that the UV light is produced mostly by the main-sequence stars in the range from about B5 to late F types. This case is well described by the μ-models, with μ from 0.5 to 0.7. Thus, the latter models do not require the presence of an HB population in order to reproduce the UV spectrum of elliptical galaxies. However, it would be surprising if star formation were uniform over the inner spheroid of elliptical galaxies (Gunn, Stryker, and Tinsley 1981).

The HB population is known to exist in galactic globular clusters. The average *IUE* UV spectra of metal-poor and metal-rich globular clusters are shown in Figure 8 of Bruzual (1981*a*) and in Paper II. The similarity of the metal-rich cluster spectrum with that of nearby elliptical galaxies is quite noticeable. This supports the assumption that the missing UV light is provided by a known population. As noted by Bruzual and Spinrad (1981) no more than a red HB population (not hotter than F0) is required to reproduce the UV in the range 2000–3200 Å.

The theoretical understanding of the evolution of stars both toward and away from the HB is far from complete. Ciardullo and Demarque (1978) have suggested that blue HB stars may originate even in a metal-rich old stellar population if enough mass is lost from the star at some stage in the red-giant phase. The tendency seems to be toward stars of lower mass evolving into bluer HB stars. The dependence on metallicity is translated into a dependence of mass loss on metal content. This effect might, possibly, outweigh the reddening due to stellar evolution and make galaxies become bluer as they get older (Ciardullo and Demarque 1978). This could, conceivably, be the case of why galaxies with redshifts in the range 0.2–0.3 are redder than models predict (see below).

Because of the lack of evolutionary tracks for HB stars, these stages have not been included in the evolutionary scheme used to build the current models (and those of authors using evolutionary synthesis). To make up for this deficiency, we have used the following ad hoc scheme. Once an age (t_g) has been chosen as the typical galaxy age, the number of stars on the HB (i.e., stars in spectral groups from A0 to F8 and of 0.4 absolute visual magnitude) that must be added to the model s.e.d. at that age to reproduce the observed galaxy spectrum is computed by trial and error. The problem that arises then is how to follow the past evolution of these HB stars, since essentially it is not known where they originated. Two possible approaches that have been considered in this work are:

1. Express the total number of HB stars needed at time t_g in terms of the number of red giants present in the model at that age, and then assume that at all ages the same proportion of stars goes into the HB. This is equivalent to redefining the red-giant luminosity function of Tinsley and Gunn (1976) to include some evolutionary stages on the HB. Since the IMF (eg. [2]) implies that there are more low-mass stars than massive ones, this scheme adds to the models an increasing (in time) amount of UV light. This estimate can be taken as an upper limit for the amount of UV light coming from the HB stars (and also for the number of them present) in the sense that not all of the UV light has to come from these stars. This approximation represents HB stars that come from an old metal-rich population (under the assumption that a fixed fraction of them evolves into the HB).

2. Assume that the amount of light provided by the HB at time t_g, and hence the number of stars in the HB, remains constant throughout the evolution of the model. This could represent a fixed underlying metal-poor population. This scheme produces models that are bluer in the past than those obtained with the previous scheme. The amount of UV light that must be added to the models at time t is an increasing function of time. In this scheme at any time $t < t_g$ we add the same amount of UV light that is needed at $t = t_g$. As before, this scheme represents an upper limit for the amount of light coming from the HB stars.

The fraction of V light required from HB stars to reproduce the UV spectrum of elliptical galaxies from 1300 to 3200 Å is given in Table 5. The data correspond to the *c*-model at three possible galaxy ages. Galaxies like NGC 4486 (M87) require a higher contribution from HB stars than normal elliptical galaxies do. For example, to reproduce the *IUE* spectrum of this galaxy presented by Perola and Tarenghi (1980), the fraction of V light needed from the HB stars at $t = 16$ is 40% higher than for a normal elliptical galaxy (see last column of Table 5). The fit to the observed spectrum from 2000 to 8000 Å is equally good after the addition of the required amount of HB light at any age. Thus, it does not seem possible to derive the typical age of the

TABLE 5

CONTRIBUTION OF DIFFERENT STELLAR GROUPS TO THE V FLUX

Group	Galaxy Age Turnoff	(1) 9 G5	(1) 13 G7	(1) 16 G9	(2) 16 G9
B5–A5 (HB)		0.005	0.01	0.02	0.05
A6–F8 (HB)		0.045	0.08	0.11	0.13
Turnoff–M6 V		0.440	0.39	0.34	0.33
Red giants		0.510	0.52	0.53	0.49

NOTE.—(1) Normal elliptical galaxy; (2) M87.

population on spectral grounds solely. Addition of the HB light ensures an almost perfect fit to the s.e.d. shown in Figure 1. It is worth pointing out that the Mg II λ2800 feature is reproduced better by the models after the addition of the HB stars than otherwise. This happens because the Mg II feature is strong in absorption in late A to early G type stars, whereas it is filled in or in emission in most of the late G and K giants in our sample (due to chromospheric activity). Without the HB stars, the red giants dominate the spectrum at 2800 Å.

b) *Indicators of Spectral Evolution*

Clearly, the best indication of evolution or lack of evolution in the spectrum of a galaxy is provided by the direct comparison of the present age spectrum with that of a similar system seen at some past epoch. Thus by comparing the s.e.d.'s of nearby elliptical galaxies with those of distant ones (involving sizable light-travel times), we expect to derive some information about spectral evolution. I have performed this comparison at three different levels: (*a*) comparison of the s.e.d.'s as a whole over a large wavelength range, (*b*) comparison of the amplitude of different spectral discontinuities known to change smoothly from one spectral type to another (and hence indicating the dominant spectral type at a given time), (*c*) color evolution, i.e., comparison of galaxy colors at redshift z with those at $z = 0$. It should be pointed out that these three indicators are not independent; differences in colors reflect differences in the amplitudes of spectral discontinuities or different slopes in the s.e.d.'s. However, since not all of these quantities are known with the same reliability for all galaxies for which data are available, I decided to present the predictions for the three indicators.

i) *Differences in Spectral Energy Distributions*

Spinrad (1977, 1980) has reviewed the available information about evolving galaxy spectra. Bruzual (1981*a*) and Bruzual and Spinrad (1981) have shown a comparison of four different early-type galaxy spectra with redshifts 0, 0.2, 0.5, and 1.1, shifted back to the galaxy rest frame. Figure 2 contains the same data as in Bruzual and Spinrad in the form of F_λ versus λ in the galaxy rest frame (*solid lines*). For comparison, the s.e.d.'s (*dashed lines*) corresponding to a $\mu = 0.7$ model at $t = 6$, 10, 13, and 16 (*top to bottom*) are shown in the same scale. In the region $\lambda < 4000$ Å the s.e.d. at $t = 16$ is shown as a light solid line. The time steps indicated in the figure have been computed for $H_0 = 50$, $q_0 = 0$. No HB population has been added (apparent from the s.e.d. at $z = 0$) since the uncertainties in its evolution would render this comparison less reliable. The trend in the model evolution reproduces the trend in the observed galaxy spectra. However, there is more spectral detail present in the models than in the observed s.e.d.'s. In order to increase the signal-to-noise ratio, the observed fluxes are averaged every 100 to 200 Å. This has the effect of diluting most of the spectral features. The continuum level and slope are preserved, as well as certain spectral discontinuities (e.g., at $\lambda = 2900$ Å). At the short-wavelength end the observed data are of poorer quality due to the faintness of the galaxies, typically 23rd magnitude in the blue. The apparent feature around 2800 Å for the $z = 0.2$ and 0.5 galaxies is not the Mg II feature and is just produced by noise in the data.

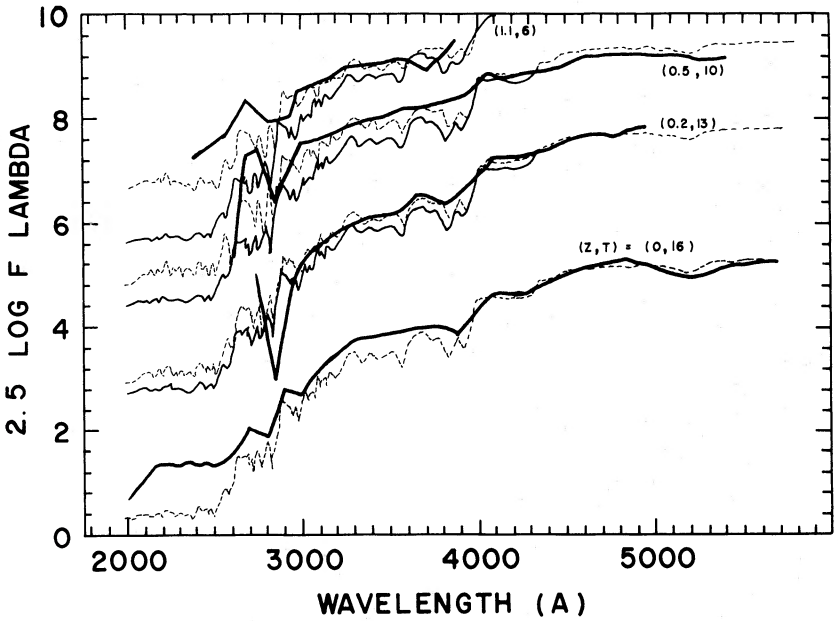

FIG. 2.—Observed spectral energy distributions (*solid lines*) for galaxies at $z = 0$, 0.2, 0.5, and 1.1 in the rest frame of the galaxies. The dashed lines represent model predictions for a $\mu = 0.7$ model with $x = 1.35$ at ages 6, 10, 13, and 16 Gyr. Each pair of spectra is labeled with the observed redshift and the assumed age. In the region $\lambda < 4000$ Å the s.e.d. at $t = 16$ is shown as a light solid line (see text).

The model s.e.d.'s have been chosen at the age in which they most closely match the observed s.e.d.'s. The galaxies at $z = 0.5$ and 1.1 are bluer in the range 2700–3800 Å than the average nearby elliptical galaxy (as can be seen by comparing the model at the given age with that at $t = 16$, i.e., *dashed and light solid lines* in Fig. 2). Similarly, the amplitude of the 4000 Å discontinuity is lower in distant galaxies than in nearby ones (see below). The same comparison can be performed with the *c*-model with essentially the same results, even though the particular ages chosen may be different.

ii) *Amplitude of Spectral Discontinuities*

Inspection of the s.e.d.'s of stars of different spectral types reveals some systematic trends in the amplitudes of different spectral discontinuities. The discontinuities are produced by the accumulation of a large number of spectral lines in a narrow wavelength region, producing a sharp opacity edge which reflects itself as a discontinuity or break in the spectrum. The elements contributing to the opacity are usually ionized metals, which explains the behavior of the discontinuities with stellar temperature. For hot stars the elements are multiply ionized, and the opacity decreases. For cool stars the temperature is too low to ionize the neutral atoms to the appropriate degree, producing again a low opacity. At some intermediate temperature the situation is optimal for a maximum degree of ionization to the appropriate stages, and the discontinuity is largest.

Four spectral discontinuities, occurring at 2420, 2640, 2900, and 4000 Å, were considered by Bruzual (1981*a*). Of these, the 4000 Å discontinuity is the one for which more galaxy data are available and is the only one that will be described in detail in this work.

The definition of the amplitude of the discontinuity is based on the visual procedure that has been used to measure it in the observed galaxy spectra. This procedure amounts to estimating the average fluxes inside a wavelength interval at the long-, $\langle F^+ \rangle$, and at the short-wavelength side, $\langle F^- \rangle$, of the spectral discontinuity (for example, to the right and left of $\lambda = 4000$ Å). In all cases the 4000 Å discontinuity was measured in galaxy spectra plotted as F_ν versus λ. In this case

$$\langle F \rangle = \frac{\int_{\lambda_1}^{\lambda_2} F_\nu d\lambda}{\int_{\lambda_1}^{\lambda_2} d\lambda}, \tag{10}$$

and the amplitude of the discontinuity is then defined as

$$D(4000) = \frac{\langle F^+ \rangle}{\langle F^- \rangle} = \frac{(\lambda_2^- - \lambda_1^-) \int_{\lambda_1^+}^{\lambda_2^+} F_\nu d\lambda}{(\lambda_2^+ - \lambda_1^+) \int_{\lambda_1^-}^{\lambda_2^-} F_\nu d\lambda}, \tag{11}$$

where $(\lambda_1^-, \lambda_2^-, \lambda_1^+, \lambda_2^+) = (3750, 3950, 4050, 4250)$ Å for the 4000 Å discontinuity.

Figure 3 shows the behavior of the 4000 Å discontinuity for stars of different spectral types. The same stellar spectra used in the population synthesis have been used to compute the amplitudes shown in this figure. It is clear that the value of any of these amplitudes for a given stellar type is sensitive to the metal abundance, being lower, in general, for stars of lower metallicity (cf. Figs. 8*a* and 8*c* of Bruzual 1981*a* and Paper II). This effect makes these amplitudes sensitive to radial metallicity gradients known to exist in elliptical galaxies. One expects that as a given aperture covers a larger fraction of a distant galaxy than of a nearby one, the contribution of low-metal abundance stars to the distant galaxy light gets more significant and tends to make the galaxy look bluer, or, equivalently, to decrease the amplitude of the discontinuities. This is the same effect expected from an aging stellar population, and until more realistic models that include both chemical and dynamical evolution as well become available, not much can be done to handle this problem theoretically. Only the use of large enough apertures, or of variable aperture

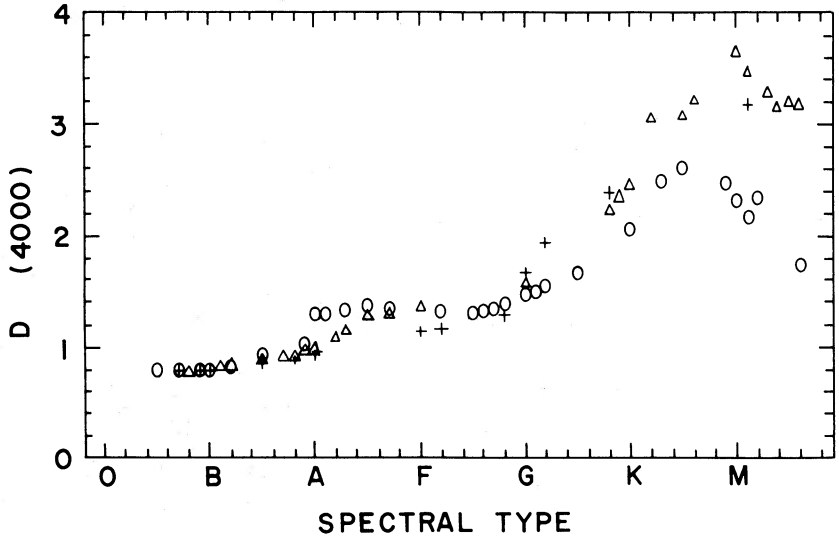

FIG. 3.—Behavior of the 4000 Å discontinuity with spectral type. Different symbols represent stars of different luminosity classes: main sequence (*circles*), giants (*triangles*), and supergiants (*crosses*).

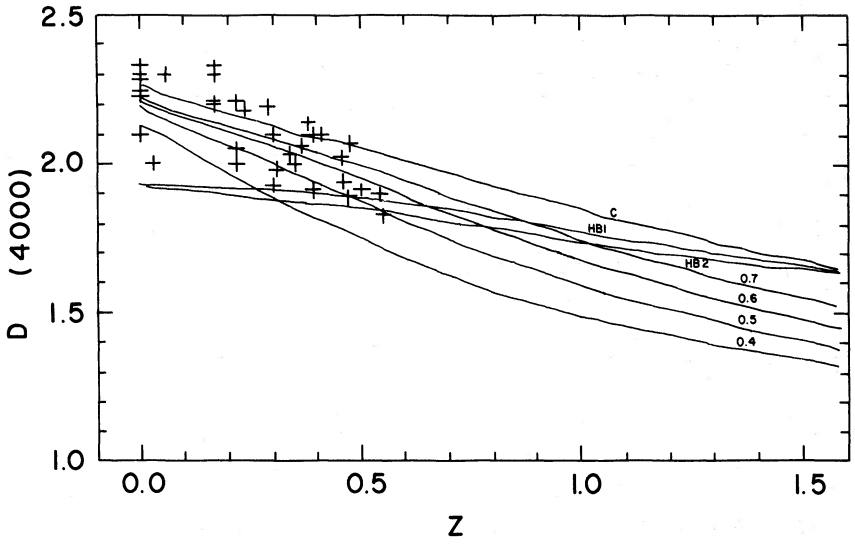

FIG. 4*a*

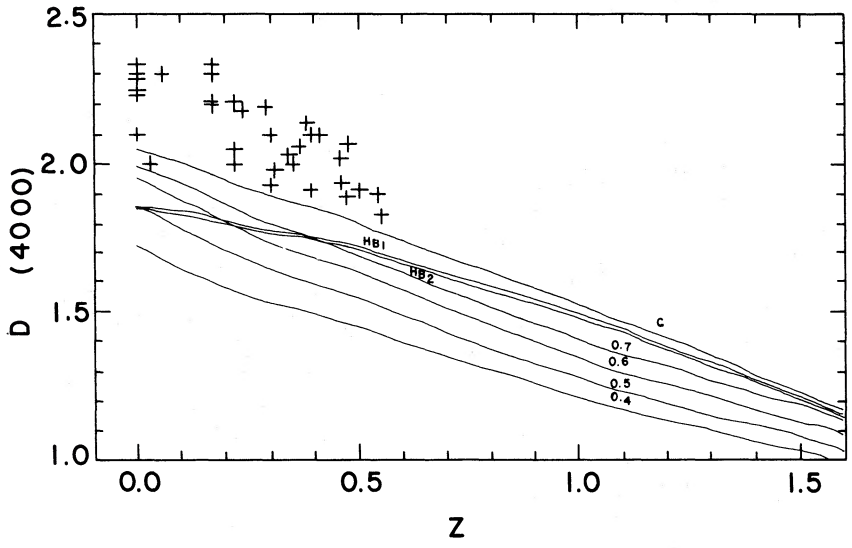

FIG. 4*b*

FIG. 4.—Comparison of model predictions and observations for the 4000 Å discontinuity. The curve marked *c* refers to the *c*-model ($\tau = 1$); curves HB1 and HB2, to the *c*-model when light from horizontal-branch stars is added according to the two different schemes described in the text. The other curves correspond to μ-models, with the value of μ indicated next to the curves. (*a*) $H_0 = 50$, $q_0 = 0$, $t_g = 16$. (*b*) $H_0 = 100$, $q_0 = 0$, $t_g = 9$. The data points were measured by the author from IDS (image dissector scanner) spectra obtained by Dr. H. Spinrad. The point near $z = 1$ (Bruzual 1981*a*) is not shown because in the meantime the redshift for that particular galaxy has been revised to a lower value (H. Spinrad, private communication).

sizes, will ensure that past a given angular size, the same fractions of different galaxies are contributing to the received signal (see below for an order of magnitude estimate of the effect of this color gradient on the observed galaxy colors).

Figure 4 contains the predicted changes in the amplitude of the 4000 Å discontinuity as a function of galaxy redshift. Two possible galaxy ages and values of H_0 have been used: $H_0 = 50$ for $t_g = 16$, and $H_0 = 100$ for $t_g = 9$. The value of q_0 has been taken as zero. In both cases the predictions for the *c*-model ($\tau = 1$) with and without HB stars, and μ-models with $\mu = 0.4$, 0.5, 0.6, and 0.7, all with $x = 1.35$, are shown. The values of the spectral discontinuities have been measured manually in plots of F_ν versus λ kindly provided by Dr. H. Spinrad. The model prediction shows the same trend as the observed data. Some of the data points are reproduced better by models with $\mu = 0.4$–0.5. These models have a continuing significant amount of star formation and in the UV are significantly brighter than observed nearby elliptical galaxies (cf. Fig. 9 of BK for a comparison; note that the model shown there has

$\mu = 0.3$, and hence it is somewhat more extreme). The predictions for $t_g = 9, H_0 = 100$ are significantly different from the ones for $t_g = 16, H_0 = 50$. The amplitude of the 4000 Å discontinuity is more sensitive to age than is a color like $B-V$ (see below). Note that the addition of the HB light to the *c*-model changes D (4000) at $z = 0$ by an appreciable amount.

As will be seen in the following section, these low-μ models ($\mu < 0.5$) predict bluer colors than observed in nearby galaxies, and it is not clear why the amplitude of this discontinuity is reproduced best by them. This may indicate that some metallicity differences are important, which will decrease the amplitude of the discontinuities without changing the observer's frame colors by as large an amount as required by star formation. Finally, models with a younger age (Fig. 4*b*) predict very low values of the discontinuity, even for the *c*-model. The same comments apply to the other discontinuities, for which much less data are currently available.

iii) *Color Evolution*

This section contains a number of results for the observed color evolution, i.e., observer's frame color versus redshift, for different models and for two different cosmologies. Three different photometric systems have been chosen to compute the model predictions: the photoelectric *UBV* system, the photographic U^+J^+FN system, and the infrared *RIJHKL* system. These systems are described in § II. In Bruzual (1981*a*) predictions are presented in both tabular and pictorial form for all the colors listed in Table 4. For reasons of space, in this paper I will present predictions in the form of plots for those colors for which a significant number of observations are available. The predictions, in the form of tables, for all the colors in Table 4 are included in Bruzual (1983*b*, hereafter Paper IV).

Because of the current uncertainties in the value of H_0, it was decided to present the results for $H_0 = 50$ and $H_0 = 100$. For intermediate values a linear interpolation should suffice. For every color two figures, *a* and *b*, are presented. The figures labeled *a* were computed with $H_0 = 50$, $q_0 = 0$, and $t_g = 16$; figures labeled *b*, with $H_0 = 100$, $q_0 = 0$, and $t_g = 9$. In all cases the predictions for the *c*-model ($\tau = 1$) and the $\mu = 0.7$, 0.6, and 0.5 models (all with $x = 1.35$) are shown. The predictions for the *c*-model when HB stars are added according to the two schemes described above are also included. For comparison, the colors for a nonevolving s.e.d. (that for the *c*-model at $z = 0$) at the appropriate redshift are also given. A description of the content of the figures for the three photometric systems follows. The conclusions derived from this section are presented in the last section.

UBV system.—Figure 5 shows the dependence of $B-V$ on z. The observed data points are from Kristian, Sandage, and Westphal (1978). Figure 5*d* shows clearly that at $t = 9$ the models are bluer (by about 0.2 mag) than nearby elliptical galaxies. The agreement with the data is better for models at $t = 16$ (Fig. 5*c*). Thus, based on this comparison only, $H_0 = 50$, $t_g = 16$ seems to be a better choice than $H_0 = 100$, $t_g = 9$. There is no complete and homogeneous set of data for $U-B$. Only the observed range, from $U-B = 0.45$ to 0.60, for nearby galaxies is known (de Vaucouleurs, de Vaucouleurs, and Corwin 1976). The models cover this range (see Paper IV).

U^+J^+FN system.—Figure 6 contains the predictions for the photographic J^+-F color. Very few data have been published in this system. The observed data points come from D. C. Koo, R. G. Kron, and H. Spinrad (private communications). Other comparisons of observed J^+-F color and model predictions are presented by van der Laan and Windhorst (1982*a*, 1983*a*, *b*) and by Koo (1981*a*, *b*).

RIJHKL system.—Figures 7, 8, and 9 show the predictions for the infrared $V-R$, $V-K$, and $H-K$ colors. The observed data in the $V-R$ plots are from Kristian, Sandage, and Westphal (1978). The data in the $H-K$ plots come from Lebofsky (1981). The errors in $H-K$ are larger than in other color indices; a typical error bar is shown in Figure 9. Lilly and Longair (1982) and Lilly, Longair, and McLean (1983) have presented independent comparisons of models and results in this system.

Some general comments can be made at this point about the color evolution of both models and galaxies.

Evolution is faster and more noticeable for bluer color indices than for redder ones, where blue and red refer to the range of the spectrum observed at $z = 0$. This becomes apparent when comparing the predictions for $B-V$ with those for $V-K$ (Figs. 5 and 8). Thus the discrimination between different models is easier when bluer colors are observed than in the opposite case. The predicted behavior for the evolving *c*-model and the nonevolving model (two top curves in every figure) is closer for red indices than for blue ones. This again is a consequence of the fact that galaxies evolve much faster in the UV and blue than in the red and infrared.

For the few colors for which enough data are available, the evolving s.e.d.'s reproduce the observed colors better than the nonevolving one. In some cases, such as $B-V$, μ-models with appreciable star formation are required to reproduce the observed colors of first-ranked cluster elliptical galaxies. The *c*-model after the addition of the HB light moves in the right sense with respect to the observed data, even though the fit is still better for μ-models ($\mu \sim 0.5$–0.7). Too many HB stars would have to be added to the *c*-model, changing the character of the s.e.d. at $z = 0$, in order to reproduce the observations. For $B-V$ the agreement with the data is markedly better for $H_0 = 50$, $t_g = 16$ than for $H_0 = 100$, $t_g = 9$.

For the indices J^+-F, $V-R$, $V-K$, and $H-K$, however, the fit is almost as good for both cosmologies. The differences between the predicted behaviors for the two cosmologies are larger at low values of z for blue indices such as $U-B$ and U^+-J^+. Unfortunately, no data are currently available in these bandpasses. According to the model predictions, a large sample of galaxies with $0.3 \leq z \leq 0.5$ and $U-B$, or U^+-J^+, color measured to about 0.1 mag should provide information

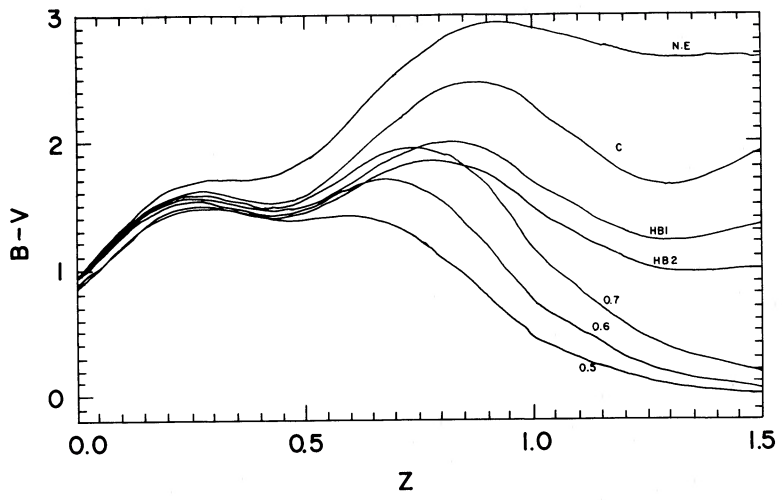

FIG. 5a

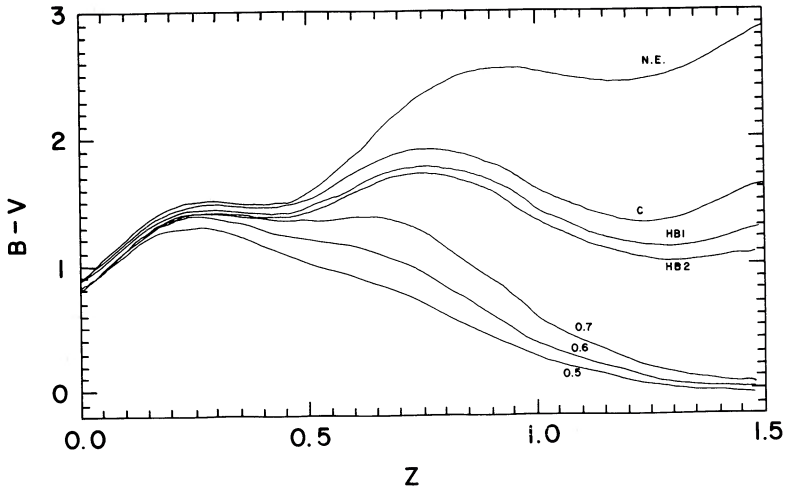

FIG. 5b

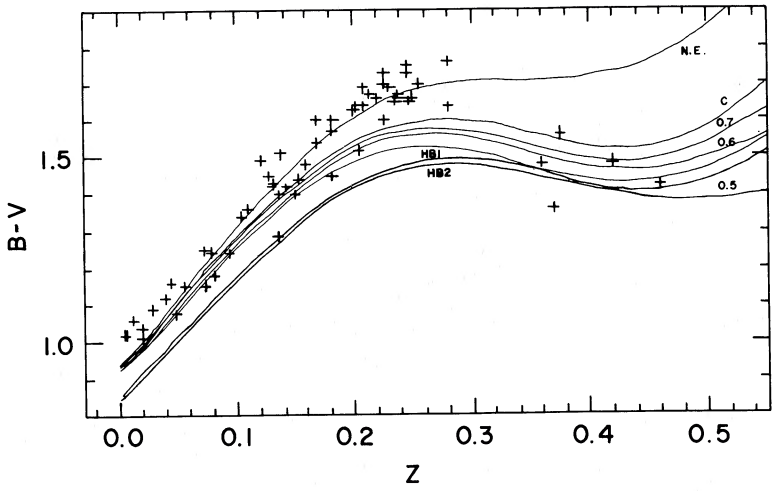

FIG. 5c

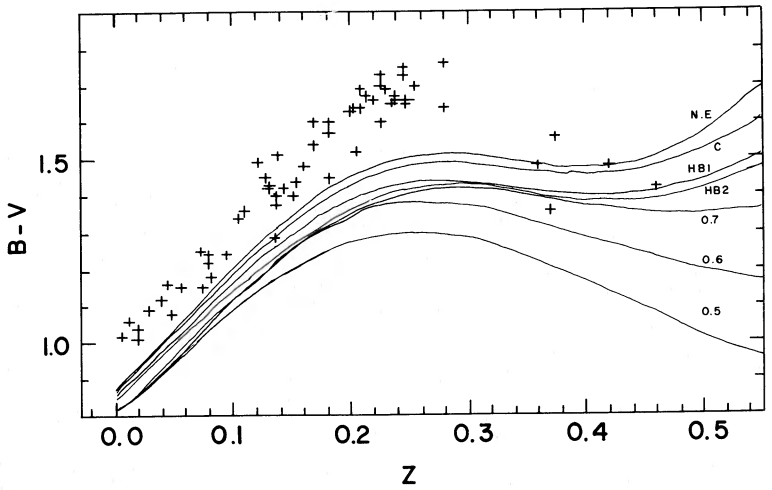

FIG. 5d

FIG. 5.—Curves of $B-V$ vs. redshift for different models. The curves marked c and N.E. (nonevolving) refer to the c-model ($\tau = 1$); curves HB1 and HB2, to the c-model when light from horizontal-branch stars is added according to the two different schemes described in the text. The other curves correspond to μ-models, with the value of μ indicated next to the curves. (*a*) $H_0 = 50$, $q_0 = 0$, $t_g = 16$. (*b*) $H_0 = 100$, $q_0 = 0$, $t_g = 9$. (*c*, *d*) Same as Figs. 5*a* and 5*b* but with an extended scale. The data points are from Kristian, Sandage, and Westphal (1978).

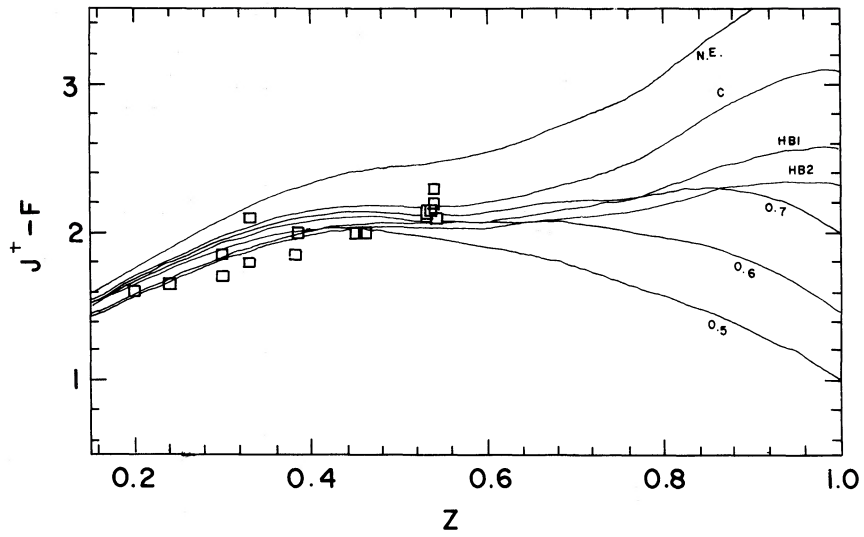

FIG. 6*a*

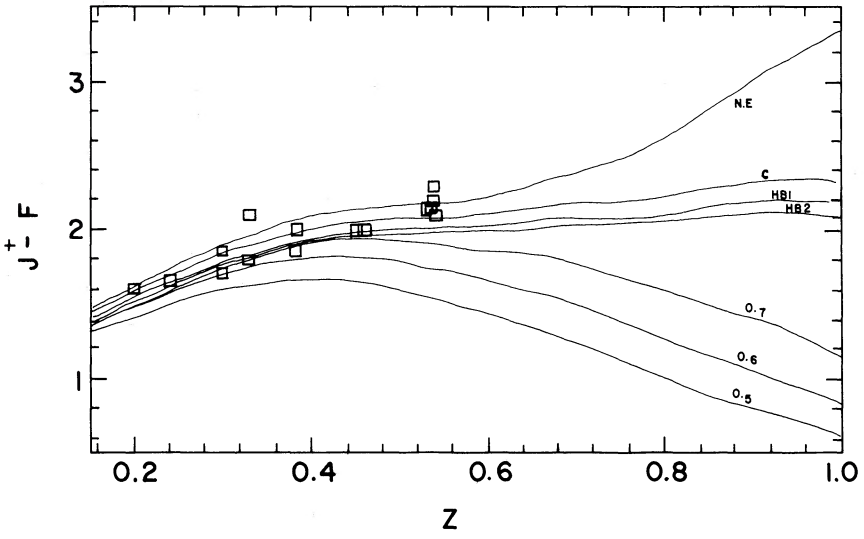

FIG. 6*b*

FIG. 6.—(*a*, *b*) Same as Fig. 5 but for $J^+ - F$. The data points are from D. C. Koo, R. G. Kron, and H. Spinrad (private communications).

about galaxy age (or H_0) and evolutionary rates. For instance, a large group of galaxies with $U-B \sim 0.2$ and $0.3 \leq z \leq 0.5$ would be explained better by the $H_0 = 100$, $t_g = 9$ cosmology than by the $H_0 = 50$, $t_g = 16$ cosmology (cf. Figs. 15 and 17 of Bruzual 1981*a*). Such galaxy samples should be available in the near future. The expected behavior for the $B-V$ index in that redshift range is very similar for both cosmologies (Fig. 5). For $z > 0.6$ the differences increase. As we go to redder colors (in the galaxy rest frame), higher values of z are required to discriminate between different cosmological models.

Oke, Bertola, and Capaccioli (1981) have argued that the observed spectral differences between nearby and distant galaxies are not due to an age effect but are instead the result of observing a larger fraction of the distant galaxies through a fixed-size aperture. Presumably, this would also explain the behavior of the 4000 Å discontinuity. However, this does not seem likely because of the following argument. The $B-V$ color of the galaxies with $z > 0.3$ in the Kristian, Sandage, and Westphal (1978) sample is in the range 1.35–1.55. This is the color range expected for the evolving s.e.d.'s used in Figure 5*c* at the appropriate redshift. On the other hand, the nonevolving s.e.d. predicts a color $B-V$ in the range 1.7–1.8 for $z > 0.3$. Thus, galaxies at $z > 0.3$ are about 0.3 mag bluer than expected just on the grounds of redshifting an observed nearby galaxy s.e.d. (see also Kristian, Sandage, and Westphal 1978). This 0.30 mag difference must be accounted for in terms of an aperture

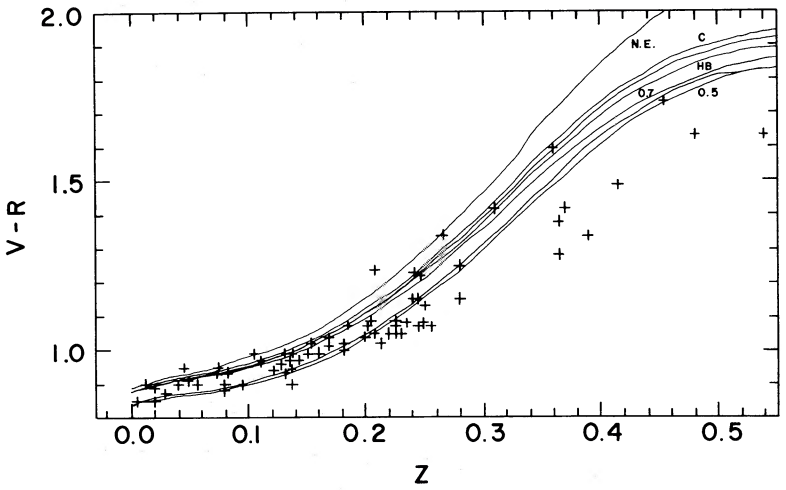

FIG. 7a

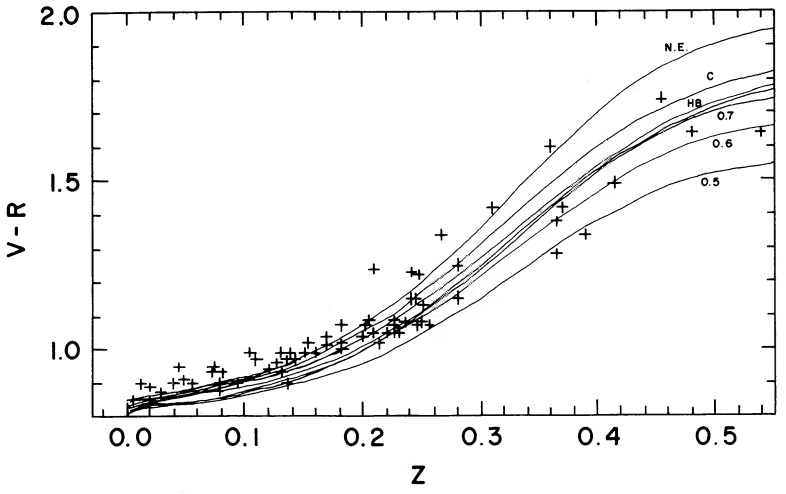

FIG. 7b

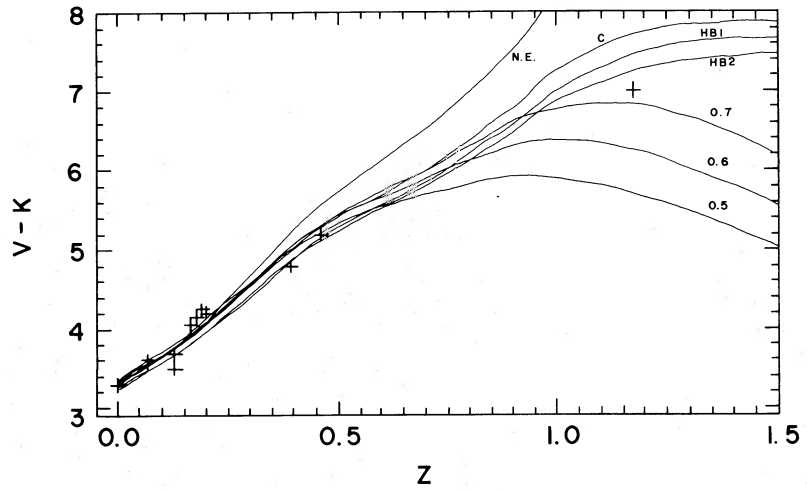

FIG. 8a

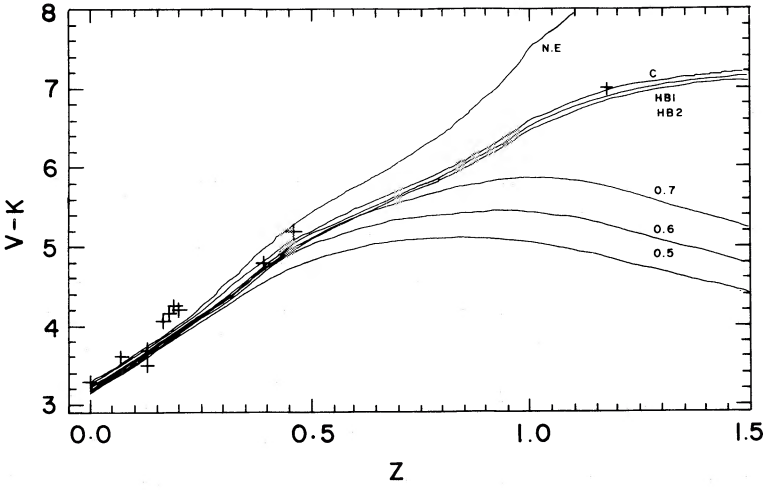

FIG. 8b

FIG. 7.—(*a*, *b*) Same as Fig. 5 but for $V-R$. The data points are from Kristian, Sandage, and Westphal (1978).
FIG. 8.—(*a*, *b*) Same as Fig. 5 but for $V-K$. The data points are from G. L. Grasdalen (private communication).

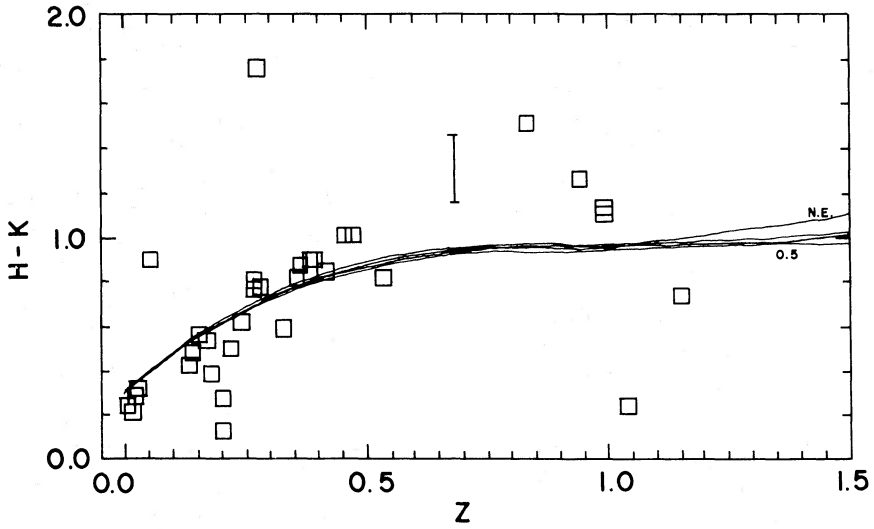

FIG. 9*a*

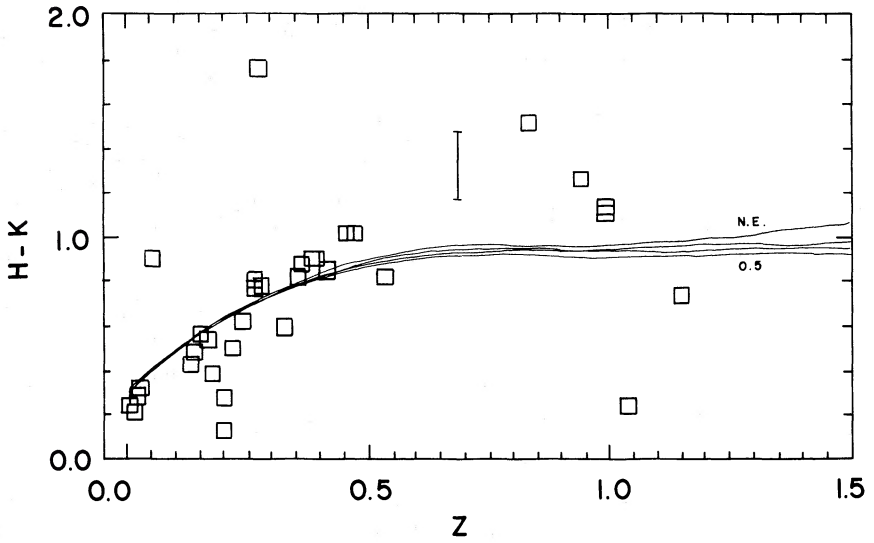

FIG. 9*b*

FIG. 9.—(*a*, *b*) Same as Fig. 5 but for $H-K$. The data points are from Lebofsky (1981).

effect. Few quantitative data are available about color gradients in galaxies, but an order of magnitude estimate of this effect can be done as follows.

Strom and Strom (1978) have performed U and R photometry of galaxies in the Coma Cluster. For NGC 4816 they find a color gradient $\Delta(U-R)/\Delta r \sim -0.02$ mag kpc^{-1} from the surface brightness profiles (reaching up to 70 kpc). H. Spinrad (1980, private communication) has performed J^+ and F photometry of the brightest galaxy in the cluster CrB 0404 at $z = 0.3$. He finds a gradient with slope ~ -0.01 mag kpc^{-1} from the J^+ and F surface brightness profiles (extending up to 50 kpc). In both cases the profiles are very similar and just show a slight difference in the slopes that translates into differences in the integrated colors. To estimate the importance of this effect we have used King's (1978) surface brightness profile of NGC 4472 in the B band. We assume that the surface brightness profile in the V band is similar to this profile but with a small distortion that introduces a gradient α mag kpc^{-1}, i.e.,

$$\sigma_B(r) = \sigma_V(r) + \alpha r ,$$

where $\alpha < 0$. By integrating both profiles up to a given radius, we find the integrated color as a function of α. In general,

$$\frac{\Delta[B(r) - V(r)]}{r} \sim 0.4\alpha ,$$

for $-0.1 \leq \alpha \leq 0$; r is measured from the origin. If we take $\alpha = -0.01$ mag kpc^{-1} as a representative value

(color gradients in $B-V$ should have a slope more similar to the gradients in J^+-F than to those in $U-R$), we have $\Delta(B-V) = -0.004r$. For a circular aperture 6″ in radius, as used by Kristian, Sandage, and Westphal (1978), we have $r = 49$ kpc at $z = 0.5$ ($H_0 = 50$, $q_0 = 0$), and the expected $\Delta(B-V)$ is ~ -0.20 mag. This is somewhat smaller than the observed difference of -0.30 mag. The s.e.d. of 3C 295 given by Gunn and Oke (1975) was obtained with an aperture of 3.″5 in radius. This s.e.d. is consistent with a $B-V$ color of 1.4 at $z = 0.461$. The argument above would predict $\Delta(B-V) \sim -0.11$ for this aperture. Thus, to explain the observed color difference of -0.30 mag as due only to a color gradient effect requires values of α 2–3 times larger (in absolute value) than have been observed.

Even though these figures are not very conclusive and are only order of magnitude estimates, it seems safe to conclude that color gradients are not large enough to explain the observed behavior of galaxy s.e.d.'s as a function of redshift, and that some spectral evolution is required. The amount of spectral evolution required if color gradients are as important as estimated above, however, is less than implied by the models (which do not consider color gradients). These estimates have been based on the model results for $t_g = 16$, $H_0 = 50$, and $q_0 = 0$. As Figure 5*d* shows, at $t = 9$ the models are too blue in $B-V$ at any redshift.

There is no detailed information about the change in the amplitude of the 4000 Å discontinuity as a function of position in a galaxy. Thus, it is not possible to repeat the arguments above for this amplitude. However, the amplitude of the 4000 Å discontinuity is well correlated with $B-V$ (Fig. 3). It is expected that if the observed color gradients in elliptical galaxies are not large enough to explain the color-redshift dependence, they will not be able to account for the observed behavior of the 4000 Å discontinuity either. The estimated color change of -0.11 mag in $B-V$ (3C 295) seems too small to bring D (4000) down from 2.3 ($z = 0$) to about 1.95 ($z = 0.46$). In the spectral range of interest, from G8 III ($B-V = 0.92$) to K6 III ($B-V = 1.54$), we find $\Delta D(4000)/\Delta(B-V) = 1.84$. The observed change of -0.35 in D (4000) requires a change of about -0.20 in $B-V$. This value is again higher than the values produced by observed color gradients, which again requires some degree of spectral evolution.

The *c*-model defines a red envelope at any redshift in the color-redshift plane. No model becomes redder than this single burst model. In all colors the reddest models (*c*, HB1, HB2, $\mu = 0.9$) always start getting bluer as soon as the epoch of appreciable star formation becomes visible. At that point the red models will look as blue as the ones that stay blue for most of their evolution. However, in all colors with enough observed data points, $B-V$, J^+-F, and $H-K$, there are galaxies with redshift in the range $z = 0.2$–0.4 that have redder colors by up to 0.2 mag than the reddest model predicts, especially in $B-V$, where the photometry is probably good. It is also true that these observed colors are redder than expected from just shifting an empirically observed giant elliptical galaxy s.e.d. (as in Whitford 1971) to the appropriate redshift (Kristian, Sandage, and Westphal 1978). The reason for this discrepancy is not clear. One possibility is that there is something wrong with the way the theoretical colors are computed. Several tests were performed, and it does not seem to be a consequence of numerical integrations or computer precision. Thus this possibility was ruled out.

A second possibility has been suggested by Ciardullo and Demargue (1978). If the contribution to the galaxy spectrum from the HB stars increases as a function of time, elliptical galaxies will show a tendency to become bluer (in their rest frame) as times goes on. This could, conceivably, explain why galaxies at $z = 0.2$–0.4 appear to be redder than nearby ones. The blueing must occur in such a way as to produce consistency at $z = 0$ for all colors. However, the time interval from $z = 0.3$ to $z = 0$ is very short (4–5 Gyr for $H_0 = 50$) for an appreciable amount of evolution to take place in the meantime, and only a particular mass range could go through this evolution.

Another possibility is that some population of very red giant stars (Faber 1977; Whitford 1980) is more significant in first-ranked cluster elliptical galaxies than in the solar neighborhood. Frogel and Whitford (1982) have presented s.e.d.'s of 20 M giants in the nuclear bulge of the Galaxy seen through "Baade's window." Their results imply that these cool giants are appreciably redder shortward of 8000 Å than local giants. Their data do not extend shortward of the B band. If this behavior is still present in the UV, and if these stars are present in large numbers in the central parts of elliptical galaxies, then one would expect the colors to look redder than the present models predict. Frogel and Whitford interpret these stars as belonging to an old super-metal-rich population. The appropriate treatment of the evolution of these stars and their effect on the spectral evolution of elliptical galaxies requires more sophisticated evolutionary tracks, as well as s.e.d.'s for these stars that extend into the UV. Similarly, evolutionary tracks that include HB evolution are needed before this discrepant behavior can be understood.

At this point it should be pointed out that the use of the empirical giant luminosity function of Tinsley and Gunn (1976) introduces some uncertainties into the models. First, there are the intrinsic uncertainties related to the possible lack of self-consistency (O'Connell 1980) and universal validity (A. Renzini, private communication) of this local luminosity function. Second, by the way this function is incorporated into the models, the spectral evolution in the red and infrared part of the spectrum is artificially stopped. The predicted much slower evolution in the infrared than at shorter wavelengths is in a way forced upon the present models, and thus it is model dependent. However, it is consistent with the observations.

c) Luminosity Evolution

Figures 10, 11, 12, and 13 show the dependence of apparent B, V, F, and K magnitudes on log z for the

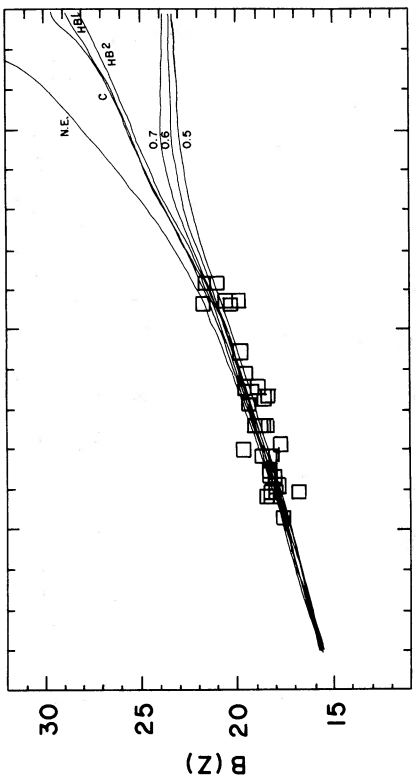

FIG. 10b

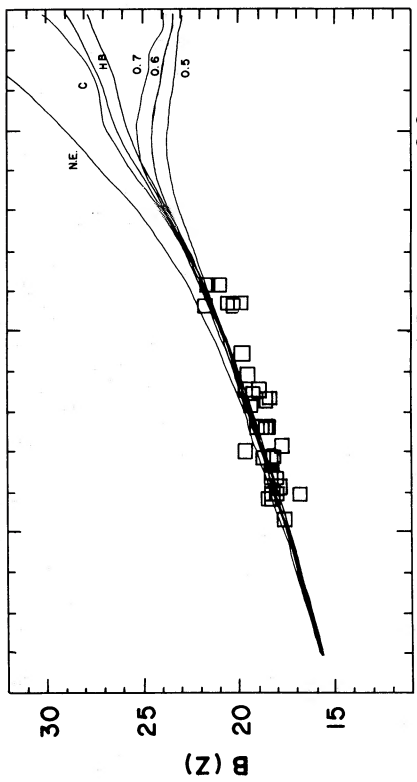

FIG. 10a

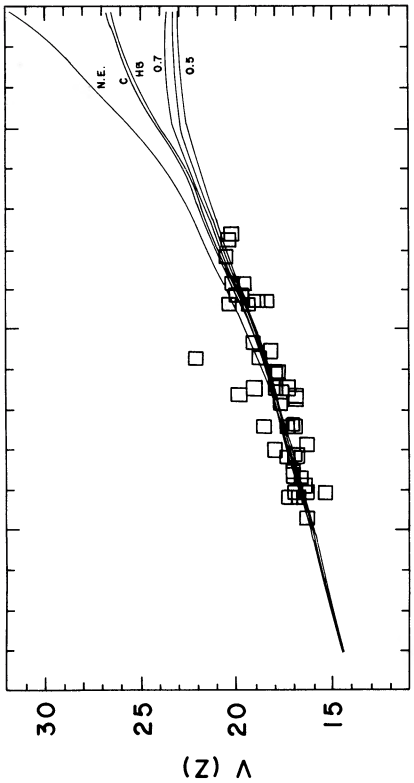

FIG. 11b

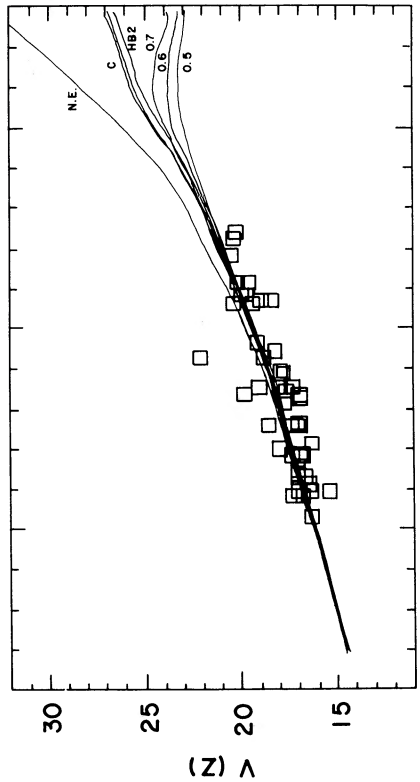

FIG. 11a

FIG. 10.—(*a*, *b*) Curves of apparent *B* magnitude vs. log *z* for the models shown in Fig. 5. All models have been normalized to an absolute magnitude of $B_0 = -22$ ($H_0 = 50$) at the present age for this figure. The data points are from Kristian, Sandage, and Westphal (1978).

FIG. 11.—(*a*, *b*) Same as Fig. 10 but for apparent *V* magnitude. Models are normalized to an absolute magnitude of $V_0 = -23$ ($H_0 = 50$) at the present age. The data points are from Kristian, Sandage, and Westphal (1978).

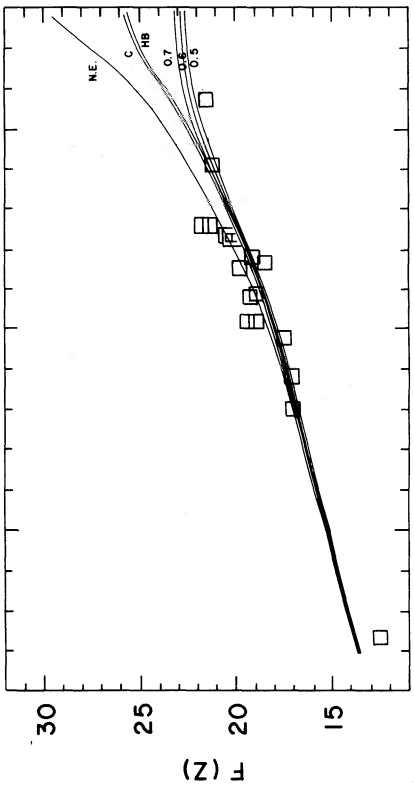

FIG. 12*a*

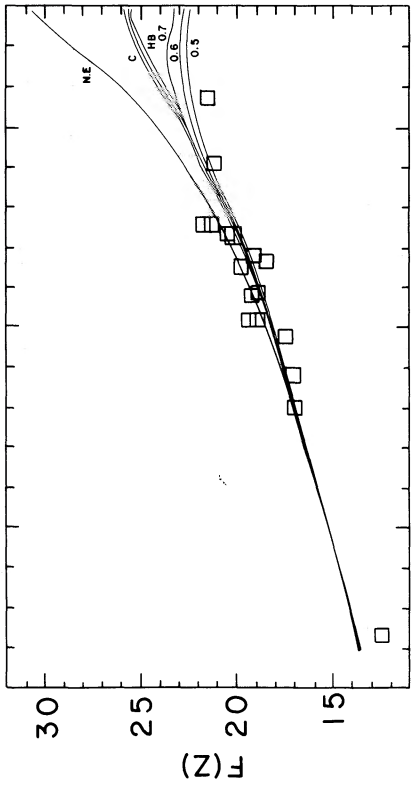

FIG. 12*b*

FIG. 13*a*

FIG. 13*b*

FIG. 12.—(*a*, *b*) Same as Fig. 10 but for apparent F magnitude. The data points are from H. Spinrad (private communication). Models are normalized to an absolute magnitude of $F_0 = -23.8$ ($H_0 = 50$) at the present age.

FIG. 13.—(*a*, *b*) Same as Fig. 10 but for apparent K magnitude. The data points are from Grasdalen (1980). Models are normalized to an absolute magnitude of $K_0 = -26.3$ ($H_0 = 50$) at the present age.

same models and cosmologies used in the previous section. These diagrams correspond to the classical Hubble diagram in the respective bandpasses. Note that since the construction of these diagrams includes both redshifting of the continuum and evolution of the stellar population in the model galaxies, it is not necessary to apply any correction to the predicted magnitudes; i.e., both the K-correction and the evolutionary correction are included in the models.

All the model s.e.d.'s have been scaled to an absolute magnitude $V_0 = -23.0$ at a distance modulus of 25 for the $H_0 = 50$ cosmology. For typical colors of $B-V = 1.0$ and $V-K = 3.3$, this corresponds to $B_0 = -22.0$ and $K_0 = -26.3$. In the F band an absolute magnitude $F_0 = -23.8$ was assigned. No attempt was made to determine the best possible absolute magnitude in each bandpass.

Comparisons of this sort are also presented by Lilly and Longair (1982) and van der Laan and Windhorst (1982*b*).

The K-correction and the evolutionary correction corresponding to these model s.e.d.'s are given in Paper IV.

V. SUMMARY AND CONCLUSIONS

In the previous sections it has been shown that simple assumptions about the SFR and the IMF in galaxies allow us to construct spectral evolutionary models of galaxies which resemble actual galaxy s.e.d.'s at various epochs.

Some important simplifying assumptions underlying these models are: (1) Galaxies can be treated as closed systems. (2) Chemical evolution is not important after the stars in galaxies are formed. Our models assume solar composition throughout. (3) The SFR is a smooth function of time (independent of stellar mass), which determines the spectral and luminosity evolution of a galaxy. (4) The IMF is a simple function of the stellar mass (independent of galaxy age) of the same general form as the IMF observed in the solar vicinity. (5) The effect of dust and gas on galaxy spectra can be neglected in a first approximation. The validity of these assumptions lies in the ability of the models to reproduce the observations.

The main results and conclusions derived from the comparison of model predictions and observations are summarized in the remainder of this section.

Models with low values of the SFR at the present epoch reproduce quite well the behavior of elliptical galaxies up to $z \sim 0.6$ (look-back time of ~ 7 Gyr for $H_0 = 50$). For larger z's very few observations are available, and the predictions cannot be adequately tested. The observed color and luminosity evolution of elliptical galaxies is reproduced better by μ-models in which a small amount of star formation takes place continuously up to the present epoch (with an exponential time decay) than by simple single burst c-models in which all the stars form during the first Gyr of the life of the galaxy.

For nearby galaxies this small amount of star formation has the same effect on the galaxy colors and s.e.d.'s as the addition of a horizontal-branch population to a metal-rich red-giant population. The effect is to increase the amount of light emitted shortward of 4000 Å. However, for distant galaxies ($z \sim 0.5$) evolving according to a μ-model ($\mu \sim 0.5$–0.7), the effect of the SFR is appreciably larger than for nearby galaxies. Main-sequence stars dominate the spectrum of these distant galaxy models in the region 3000–4000 Å (observed at $z = 0.5$ in $B-V$ or J^+-F, for instance). Models without star formation going on at that epoch are much redder in $B-V$ than any observed galaxies. The number of horizontal-branch stars required to reproduce the spectrum at $z = 0.5$ is larger than expected in nearby galaxies. However, the evolutionary path of horizontal-branch stars in the H-R diagram is not well known at the present time. It would be premature to conclude on these grounds solely that at $z = 0.5$ the UV light comes mostly from stars on the main sequence (A, F type stars) rather than from horizontal-branch stars. A deeper theoretical understanding of the horizontal-branch stars is required before such a conclusion can be established. However, models based on this conclusion are consistent with observational data.

The behavior of early-type galaxies in clusters of galaxies is well understood in terms of models with $\mu = 0.6$–0.7. Koo (1981*a*, *b*) has established a sequence of clusters up to $z = 0.54$ with U^+J^+FN photographic photometry whose behavior is well reproduced by these models.

The situation for late-type systems is not so clear. UV observations of nearby spiral galaxies are very scarce and in some cases do not show the anticipated systematic trends with the optically observed colors. Models that at the present time have relatively large (with respect to an average rate) values of the SFR have optical colors in the observed range for spiral galaxies. However, if stars form according to a Salpeter IMF with a single value of x for all values of the stellar mass, low values of x ($x < 1$) are required. For small x the fraction of low-mass stars is decreased. Low-mass stars, once they become red giants, will dominate the galaxy spectrum. If large numbers of them are produced, the model will resemble an elliptical galaxy when it is old. Low values of x produce relatively large numbers of massive stars which dominate the UV galaxy spectrum.

The most critical spectral region for comparison seems to be from 2000 to 4000 Å. Shortward of 2000 Å the spectrum is dominated by O and B type stars, and it appears similar for any value of x. For a given SFR the ratio of the flux at 2500 Å with respect to the flux at 4000 Å is a strong function of x. This ratio increases as x decreases. The uncertainties in the model and observed s.e.d.'s in this region do not allow the derivation of any definitive conclusion about this problem. However, models with a mass-dependent slope in the IMF reproduce better the UV spectrum of nearby spiral galaxies. The required values of x are in reasonable agreement with observations in the solar vicinity.

The spectral region from 2000 to 4000 Å is observed

in optical colors for galaxies with $z \sim 0.5$ $(U-B)$ or $z \sim 0.9$ $(B-V)$. The tendency is for the predicted $U^+ - J^+$ color to be bluer (up to 0.5 mag) than the scarce photographic color data indicate (Koo 1981*b*).

It is expected that a large sample of galaxies with well-known z's and precisely measured colors will improve our knowledge about galaxy spectra and color distributions as a function of z and apparent magnitude.

Detailed models for late-type systems will be considered in a future paper in this series.

I want to thank Dr. Hyron Spinrad for suggesting this thesis topic. His continuous interest in this subject kept my motivation alive and helped me bring my work to completion. I also thank Drs. David Koo and Richard Kron for providing me with their valuable data before publication, as well as for their continuous interest in my work; and Dr. Ivan King for his careful reading of my manuscripts. I also thank those people in the Berkeley Astronomy Department and elsewhere who helped and supported me on many occasions.

I would like to thank Dr. Beatrice Tinsley for her interest in my work, and her willingness to share and compare our results. I appreciated her generous collaboration in a subject that she pioneered. I regret her untimely death.

I gratefully acknowledge financial support from the Berkeley Astronomy Department, the Consejo Nacional de Investigaciones Científicas y Tecnológicas (CONICIT, Venezuela), and the Centro de Investigaciones de Astronomía (CIDA, Venezuela).

REFERENCES

Alcock, C., and Paczyński, B. 1978, *Ap. J.*, **223**, 244.
Arvesen, J. C., Griffin, R. N., and Pearson, B. D. 1969, *Appl. Optics*, **8**, 2215.
Ažusienis, A., and Straižys, V. 1969, *Soviet Astr.—AJ*, **13**, 316.
Bertola, F., Capaccioli, M., Holm, A. V., and Oke, J. B. 1980, *Ap. J. (Letters)*, **237**, L65.
Bertola, F., Capaccioli, M., and Oke, J. B. 1982, *Ap. J.*, **254**, 494.
Broadfoot, A. L. 1972, *Ap. J.*, **173**, 681.
Bruzual A., G. 1981*a*, Ph.D. thesis, University of California, Berkeley. (Available from University Microfilms International, Ann Arbor, Mich. 48106, USA.)
———. 1981*b*, *Rev. Mexicana Astr. Ap.*, **6**, 19.
———. 1983*a*, *Rev. Mexicana Astr. Ap.*, **8**, 29. (Paper II).
———. 1983*b*, *Rev. Mexicana Astr. Ap.*, **8**, 63. (Paper IV).
Bruzual A., G., and Kron, R. G. 1980, *Ap. J.*, **241**, 25 (BK).
Bruzual A., G., Peimbert, M., and Torres-Peimbert, S. 1982, *Ap. J.*, **260**, 495.
Bruzual A., G., and Spinrad, H. 1981, in *The Universe at Ultraviolet Wavelengths: The First Two Years of IUE*, ed. R. D. Chapman (NASA CP-2171).
Buser, R. 1978, *Astr. Ap.*, **62**, 411.
Chiosi, C., Nasi, E., and Sreenivasan, S. F. 1978, *Astr. Ap.*, **63**, 103.
Ciardullo, B., and Demarque, P. 1977, *Trans. Astr. Obs. Yale Univ.*, Vol. **33**.
———. 1978, in *IAU Symposium 80, The HR Diagram*, ed. A. G. D. Philip and D. S. Hayes (Dordrecht: Reidel), p. 345.
Code, A. D., and Meade, M. R. 1979, *Ap. J. Suppl.*, **39**, 195.
Code, A. D., and Welch, G. A. 1982, *Ap. J.*, **256**, 1.
de Vaucouleurs, G., de Vaucouleurs, A., and Corwin, H. G. 1976, *Second Reference Catalogue of Bright Galaxies* (Austin: University of Texas Press).
Faber, S. M. 1972, *Astr. Ap.*, **20**, 361.
———. 1977, in *The Evolution of Galaxies and Stellar Populations*, ed. B. M. Tinsley and R. B. Larson (New Haven: Yale University Observatory), p. 301.
Flower, P. J. 1977, *Astr. Ap.*, **54**, 31.
Frogel, J. A., and Whitford, A. E. 1982, *Ap. J. (Letters)*, **259**, L7.
Grasdalen, G. L. 1980, in *IAU Symposium 92, Objects of High Redshift*, ed. G. O. Abell and P. J. E. Peebles (Dordrecht: Reidel), p. 257.
Gunn, J. E. 1982, in *Astrophysical Cosmology: Proceedings of the Study Week on Cosmology and Fundamental Physics*, ed. H. A. Brück, G. V. Coyne, and M. S. Longair (Vatican City: Pontificia Academia Scientiarum), p. 233.
Gunn, J. E., and Oke, J. B. 1975, *Ap. J.*, **195**, 255.
Gunn, J. E., Stryker, L. L., and Tinsley, B. M. 1981, *Ap. J.*, **249**, 48.
Huchra, J. 1977, *Ap. J.*, **217**, 928.
Iben, I. 1967, *Ann. Rev. Astr. Ap.*, **5**, 571.
Johnson, H. L. 1965, *Ap. J.*, **141**, 923.
———. 1966, *Ann. Rev. Astr. Ap.*, **4**, 193.
King, I. R. 1978, *Ap. J.*, **222**, 1.
Koo, D. C. 1981*a*, Ph.D. thesis, University of California, Berkeley.
———. 1981*b*, *Ap. J. (Letters)*, **251**, L75.
Kristian, J., Sandage, A., and Westphal, J. A. 1978, *Ap. J.*, **221**, 383.
Kron, R. G. 1978, Ph.D. thesis, University of California, Berkeley.
———. 1980, *Phys. Scripta*, **21**, 652.
Kurucz, R. 1979, *Ap. J. Suppl.*, **40**, 1.
Lebofsky, M. J. 1980, in *IAU Symposium 92, Objects of High Redshift*, ed. G. O. Abell and P. J. E. Peebles (Dordrecht: Reidel), p. 257.
———. 1981, *Ap. J. (Letters)*, **245**, L59.
Lilly, S. J., and Longair, M. S. 1982, in *Astrophysical Cosmology: Proceedings of the Study Week on Cosmology and Fundamental Physics*, ed. H. A. Brück, G. V. Coyne, and M. S. Longair (Vatican City: Pontificia Academia Scientiarum), p. 269.
Lilly, S. J., Longair, M. S., and McLean, I. S., 1983, *Nature*, **301**, 488.
Macchetto, F., van de Hulst, H. C., di Serego Alighieri, S., and Perryman, M. A. C. 1980, in *The Faint Object Camera for the Space Telescope* (Paris: European Space Agency).
Nørgaard-Nielsen, H. U., and Kjaergaard, P. 1981, *Astr. Ap.*, **93**, 290.
O'Connell, R. W. 1976, *Ap. J.*, **206**, 370.
———. 1980, *Ap. J.*, **236**, 430.
Oke, J. B., Bertola, F., and Capaccioli, M. 1981, *Ap. J.*, **243**, 453.
Pence, W. 1976, *Ap. J.*, **203**, 39.
Perola, G. C., and Tarenghi, M. 1980, *Ap. J.*, **240**, 447.
Persson, S. E., Frogel, J. A., and Aaronson, M. 1979, *Ap. J. Suppl.*, **39**, 61.
Pritchet, C. 1977, *Ap. J. Suppl.*, **35**, 397.
Roberts, M. S. 1975, in *Stars and Stellar Systems*, Vol. **9**, *Galaxies and the Universe*, ed. A. Sandage, M. Sandage, and J. Kristian (Chicago: University of Chicago Press), p. 309.
Salpeter, E. E. 1955, *Ap. J.*, **121**, 161.
Searle, L. 1972, in *IAU Colloquium 17, L'Ages des etoiles*, ed. G. Cayrel de Strobel and A. M. Delplace (Meudon: Observatoire de Paris), p. LII.
Searle, L., Sargent, W. L. W., and Bagnuolo, W. G. 1973, *Ap. J.*, **179**, 427.
Seaton, M. J. 1979, *M.N.R.A.S.*, **187**, 73p.
Serrano, A. 1978, Ph.D. thesis, University of Sussex.
Spinrad, H. 1977, in *The Evolution of Galaxies and Stellar Populations*, ed. B. M. Tinsley and R. B. Larson (New Haven: Yale University Observatory), p. 301.
———. 1980, in *IAU Symposium 92, Objects of High Redshift*, ed. G. O. Abell and P. J. E. Peebles (Dordrecht: Reidel), p. 39.
Spinrad, H., and Taylor, B. J. 1971, *Ap. J. Suppl.*, **22**, 445.
Straižys, V., and Sviderskiene, Z. 1972, *Bull. Vilnius Astr. Obs.*, **35**, 1.
Strom, K. M., and Strom, S. E. 1978, *A.J.*, **83**, 73.
Tinsley, B. M. 1967, Ph.D. thesis, University of Texas, Austin.
———. 1972*a*, *Astr. Ap.*, **20**, 383.
———. 1972*b*, *Ap. J.*, **178**, 319.
———. 1977, *Ap. J.*, **211**, 621; erratum 1977, *Ap. J.*, **216**, 349.

Tinsley, B. M. 1978, *Ap. J.*, **222**, 14.
———. 1980*a*, *Fund. Cosmic Phys.*, **5**, 287.
———. 1980, *Ap. J.*, **241**, 41.
Tinsley, B. M., and Gunn, J. E. 1976, *Ap. J.*, **203**, 52.
Turnrose, B. E. 1976, *Ap. J.*, **210**, 33.
van der Laan, H., and Windhorst, R. H. 1982*a*, in *Astrophysical Cosmology: Proceedings of the Study Week on Cosmology and Fundamental Physics*, ed. H. A. Brück, G. V. Coyne, and M. S. Longair (Vatican City: Pontificia Academia Scientiarum), p. 263.
———. 1982*b*, in *Astrophysical Cosmology: Proceedings of the Study Week on Cosmology and Fundamental Physics*, ed. H. A. Brück, G. V. Coyne, and M. S. Longair (Vatican City: Pontificia Academia Scientiarum), p. 349.
van der Laan, Laan, H., and Windhorst, R. H. 1983*a*, in *IAU Symposium 104, Early Evolution of the Universe and Its Present Structure*, ed. G. Abell (Dordrecht: Reidel), in press.
———. 1983*b*, in *IAU Symposium 104, Early Evolution of the Universe and Its Present Structure*, ed. G. Abell (Dordrecht: Reidel), in press.
Whitford, A. E. 1971, *Ap. J.*, **169**, 215.
———. 1980, *Bull. AAS.*, **11**, 675 (abstract).
Wilkinson, A., and Oke, J. B. 1978, *Ap. J.*, **220**, 376.
Wu, C. C., Faber, S. M., Gallagher, J. S., Peck, M., and Tinsley, B. M. 1980, *Ap. J.*, **237**, 290.

Note added in proof.—The results presented in §§ IV*b* and IV*c* for a nonevolving s.e.d. (line marked N.E. in Figs. 5–13) were computed from the *c*-model s.e.d. at the indicated age and not from the average observed elliptical galaxy s.e.d. The predicted behavior for the latter will fall closer to the lines marked *c*, HB1, and HB2 in these figures. The *K*-corrections computed from the observed s.e.d. in different bands will be given in a future paper. These *K*-corrections should be preferred to the ones derived from the present paper.

G. Bruzual A.: Centro de Investigaciones de Astronomía (CIDA), Apartado Postal 264, Mérida 5101-A, Venezuela